horticulturae

MDPI

Article

Integrated Analysis of Physiological, Transcriptomic, and Metabolomic Data Reveals the Drought Response Mechanism in Cabbage

Huiru Wang [1], Yanming Gao [2,3,4], Yune Cao [2,3,4] and Jianshe Li [1,2,3,4,*]

[1] School of Civil and Hydraulic Engineering, Ningxia University, Yinchuan 750021, China; whr19995272835@163.com
[2] College of Enology and Horticulture, Ningxia University, Yinchuan 750021, China
[3] Ningxia Engineering Technology Research Center of Modern Protected Horticulture, Ningxia University, Yinchuan 750021, China
[4] Engineering Research Center for Efficient Utilization of Modern Agricultural Water Resources in Arid Regions, Ministry of Education, Ningxia University, Yinchuan 750021, China
* Correspondence: jslinxcn@163.com

Abstract

Under global climate change, cabbage (*Brassica oleracea* var. *capitata*), a major vegetable crop, is increasingly exposed to intermittent and fluctuating drought stress. A multi-level investigation of its adaptive strategies under water-deficit conditions is therefore essential for a comprehensive understanding of drought tolerance and for accelerating genetic breeding programs. In this study, the drought-resistant cultivar 'ZG-628' and the drought-sensitive cultivar 'ZG-21' were selected based on seed germination indices. Integrated physiological measurements, transcriptomic profiling, and metabolomic analyses were conducted to systematically compare their responses to drought stress. The results showed that the drought-resistant genotype 'ZG-628' maintained better water status, exhibited higher antioxidant enzyme activities, and accumulated greater levels of osmotic regulators under drought conditions. In addition, 'ZG-628' preserved higher chlorophyll content and photosynthetic efficiency than the sensitive genotype. At the molecular level, 'ZG-628' primarily responded to drought through key components of the abscisic acid (ABA) signaling pathway, including PYL, PP2C, and SnRK2. Metabolomic analysis further revealed preferential accumulation of flavonoids and ABA-related metabolites 'ZG-628', accompanied by specific activation of the "flavonoid and flavonol biosynthesis" pathway. Integrated multi-omics analysis indicated that plant hormone signal transduction was the most significantly enriched pathway among drought-responsive differentially expressed genes. Overall, this study systematically elucidates the coordinated multi-omics mechanisms underlying drought resistance in cabbage and provides both a theoretical basis and potential molecular targets for breeding drought-tolerant cabbage varieties.

Keywords: cabbage; drought stress; abscisic acid signaling; transcriptome; metabolome

Check for updates

Academic Editor: Jian Wu

Received: 30 December 2025
Revised: 5 February 2026
Accepted: 12 February 2026
Published: 16 February 2026

Copyright: © 2026 by the authors. Licensee MDPI, Basel, Switzerland. This article is an open access article distributed under the terms and conditions of the Creative Commons Attribution (CC BY) license.

1. Introduction

Drought stress represents a major constraint on crop growth and agricultural productivity, and its frequency and severity are being increasingly intensified by global climate change [1,2]. Currently, arid and semi-arid regions account for approximately 41% of the global land area, and drought-prone areas continue to expand as a result of improper irrigation practices, vegetation degradation, and other anthropogenic factors [3]. Drought

reduces available soil moisture, directly disturbing plant water balance and consequently inhibiting cell expansion, photosynthesis, and nutrient transport [4,5]. Worldwide, drought leads to substantial losses in crop yield, threatening to the production security of both grain [6], and horticultural crops [7,8], and constraining sustainable agricultural development. Under drought conditions, crops typically exhibit leaf wilting and reduced biomass, accompanied by excessive accumulation of reactive oxygen species (ROS), enhanced membrane lipid peroxidation, and impairment of the photosynthetic apparatus [9]. Therefore, elucidating the physiological and molecular mechanisms underlying crop responses to drought stress is essential for breeding drought-resistant varieties and for maintaining stable high agricultural yields.

Through long-term adaptation to arid environments, plants have evolved multi-layered response systems that integrate coordinated processes from signal perception to metabolic regulation, thereby alleviating physiological stress caused by water deficit [10]. At the onset of drought, membrane-localized receptor-like kinases and related sensors perceive changes in cellular water status and subsequently trigger intracellular signaling via second messengers such as calcium ions and ROS [11]. As both signaling molecules and stress factors, ROS rapidly accumulate during the early stages of drought and represent one of the initial events in plant stress responses; however, drought; if not effectively scavenged, excessive ROS cause severe oxidative damage [12]. ROS not only participate in regulating stomatal movement to reduce transpiration but also activate mitogen-activated protein kinase signaling pathways, which initiate downstream defense responses through phosphorylation cascades [13]. At the transcriptional level, multiple transcription factors finely coordinate drought responses [14]. Studies in wheat [15], Arabidopsis [16], and tomato [17] have shown that WRKY transcription factors are strongly induced by drought stress. These nuclear-localized proteins, many of which possess transcriptional activation activity, enhance drought resistance by mediating abscisic acid (ABA) signaling, transduction pathways, regulating stress-responsive gene expression, modulating osmolyte accumulation, enhancing antioxidant enzyme activities, scavenging ROS, and reducing malondialdehyde (MDA) levels, ultimately improving stress tolerance. Similarly, research in peanut [18], rice [19], and tomato [20] indicates that bHLH transcription factors act as positive regulators of drought tolerance. They activate antioxidant and stress-responsive genes, suppress ABA catabolism, and interact with other transcriptional regulators to coordinately strengthen drought resistance. Studies in soybean [21], and sweet potato [22] further demonstrate that NAC transcription factors function as key positive regulators of drought tolerance. These factors integrate multiple regulatory pathways by interacting with other NAC members to cooperatively activate downstream targets, modulating ubiquitination processes, and fine-tuning ABA signaling. Concurrently, they contribute to delay senescence and help maintain photosynthetic function, thereby enhancing plant performance under drought. Metabolic remodeling also represents a critical component of drought adaptation [23]. In amino acid metabolism, compatible solutes such as proline and glycine betaine accumulate to stabilize protein structures and maintain enzymatic activity [24]. In carbohydrate metabolism, elevated starch hydrolase activity promotes starch degradation into soluble sugars, which function both as osmolytes to maintain cellular water potential and as energy substrates for stress responses [25]. In secondary metabolism, compounds including flavonoids and phenolic acids markedly increase. Flavonoids [26] contribute to ROS scavenging and protection of the photosynthetic apparatus, whereas phenolic acids [27] reinforce cell walls and enhance tissue water retention capacity. Moreover, changes alterations occur in membrane lipid composition, whereby increased proportions of unsaturated fatty acids maintain membrane fluidity and integrity, thereby mitigating drought-induced membrane damage [28]. Together, these multi-layered response mech-

anisms, extensively characterized in model plants and several crops, provide a valuable theoretical framework and candidate regulatory pathways for deciphering drought tolerance in vegetable crops such as cabbage.

Under drought stress, phytohormones regulate plant responses through a complex and interactive signaling network. Jasmonic acid and salicylic acid synergistically participate in stomatal regulation and defense responses; gibberellins and ethylene jointly mediate growth inhibition; cytokinins, which are closely associated with nitrogen metabolism and leaf senescence, often antagonize other growth-promoting hormones; and brassinosteroids can independently sustain growth and osmotic balance via vascular receptor-mediated pathways. Extensive cross-talk among these hormones integrates environmental signals to balance growth and stress adaptation under drought conditions. Among them, ABA functions as the central regulator of drought responses, coordinating plant stress resistance through broad interactions with the hormone network. ABA is a key stress hormone in plant adaptation to drought and plays an essential role in drought defense mechanisms [29]. Drought stress rapidly induces ABA accumulation, which is perceived by receptors of the PYR/PYL/RCAR family [30]. ABA binding inhibits PP2C phosphatases, thereby releasing their repression of SnRK2 kinases and resulting in SnRK2 activation [31,32]. Activated SnRK2s coordinate a series of adaptive responses by phosphorylating downstream targets, including stomatal ion channels and transcription factors such as ABFs. These actions range from rapid stomatal closure to reduce water loss [33], to induction of transcription factors including NAC that regulate senescence- and stress-responsive gene expression [34,35], and to growth inhibition and optimization of resource allocation under stress [36,37]. This highly conserved core ABA signaling module and its downstream network constitute the cornerstone of regulatory mechanisms governing plant drought adaptation.

As an important leafy vegetable of the Brassicaceae family cultivated worldwide, cabbage occupies an indispensable position in both the vegetable industry and daily diets [38]. However, cabbage has high water requirements throughout its growth cycle. Drought stress severely restricts cabbage growth and development, resulting in leaf wilting, reduced biomass, yield loss, and deterioration of product quality. Consequently, drought has become a major environmental factor limiting the achievement of high-quality and high-yield cabbage production [39,40]. Identifying drought-responsive genes in cabbage and elucidating the molecular regulatory mechanisms underlying drought adaptation are therefore of great significance for improving drought resistance through genetic improvement. To date, studies on cabbage drought responses have mainly focused on physiological indicators or single-omics analyses, whereas systematic investigations using integrated multi-omics approaches remain scarce [41]. In this study, 29 cabbage varieties were used as experimental materials. A drought-tolerant genotype ('ZG-628') and a drought-sensitive genotype ('ZG-21') were screened under polyethylene glycol (PEG-6000)-simulated drought conditions. By integrating physiological assessments, transcriptomic profiling, and metabolomic analyses, we systematically characterized physiological adaptations, key differentially expressed genes (DEGs), and metabolic reprogramming in response to drought stress. In particular, the regulatory roles of core pathways, especially ABA signaling transduction, were elucidated. These findings not only fill the knowledge gap regarding multi-omics coordination underlying drought tolerance in cabbage and reveal distinct adaptive strategies between contrasting genotypes, but also provide an important theoretical basis for the molecular breeding of drought-resistant cabbage varieties.

2. Materials and Methods

2.1. Plant Materials and PEG Treatment

Twenty-nine cabbage varieties were obtained from a commercial seed company and used as initial materials for drought tolerance screening. These varieties represent common agronomic types cultivated in northern China. All tested materials were spherical early-maturing cabbages, typically requiring approximately 60 days from transplanting to harvest, and suitable for spring planting. The experiment was conducted in a temperature-controlled growth chamber in Yinchuan, China. To evaluate drought resistance during seed germination, osmotic stress was simulated using a 20% polyethylene glycol 6000 (PEG-6000) solution [42]. Fifty full, uniform, and disease-free seeds were surface-sterilized by immersion in 75% ethanol for 1 min, followed by treatment with 10% sodium hypochlorite for 15 min, and then rinsed thoroughly with sterile water three to five times. The sterilized seeds were evenly placed in 9 cm Petri dishes lined with two layers of filter paper. The treatment group received 15 mL of 20% PEG-6000 solution, whereas the control group received an equal volume of sterile water. All chemicals were supplied by Sangon Biotech (Shanghai, China). The Petri dishes were incubated in a controlled growth chamber (Ningbo Southeast Instrument, Ningbo, China) at 25 °C and 70% relative humidity. To prevent filter paper desiccation and maintain a stable osmotic environment around the seeds, 2 mL 20% PEG-6000 was added daily to compensate for water loss through evaporation.

The relative germination rate (RGR) and germination drought resistance index (GDRI) were calculated using the following equations:

$$\text{RGR} = (\text{Germination rate under stress}/\text{Germination rate under control}) \times 100\%$$

$$\text{GDRI} = \text{PI under drought stress}/\text{PI under control}$$

where PI (Peak Value) = $nd_2 \times 1.00 + nd_4 \times 0.75 + nd_6 \times 0.50 + nd_8 \times 0.25$, and nd_x denotes the number of seeds germinated on day X.

2.2. Plant Growth Conditions and Drought Stress Treatment

Seeds of the drought-tolerant cultivar 'ZG-628' and the drought-sensitive cultivar 'ZG-21' were selected based on uniformity, integrity, and absence of disease. For each cultivar and treatment (control and drought), three independent biological replicates were established. Each replicate consisted of 72 uniform seedlings grown in separate cells of seedling trays. For each cultivar, seeds were divided into two groups: a well-watered control and a drought-stressed treatment, with three biological replicates per condition. All seedlings were arranged in a completely randomized design within the greenhouse to minimize positional effects. Seeds were sown in 72-cell trays filled with a uniform nursery substrate, and all plants were maintained under consistent greenhouse conditions. From emergence to 15 days after sowing, both control and drought groups were irrigated daily at 08:00 with half-strength Yoshida nutrient solution to maintain substrate relative water content at approximately 80%. The irrigation volume was determined daily using the weighing method and typically ranged from 600 to 800 mL per tray per day. At 15 days after emergence, seedlings in the drought treatment groups were subjected to severe water deficit by adjusting and maintaining substrate relative water content at 40% using the same weighing procedure and schedule. This reduced daily irrigation to approximately 200–400 mL per tray per day. After 15 days of continuous drought treatment, at 30 days after emergence, plant samples were harvested for subsequent physiological analyses.

2.3. Determination of Physiological Parameters

Plant moisture content (PMC): Seedlings were placed in sealed bags to determine plant fresh weight (PWF). Samples were then transferred to pre-weighed kraft paper bags and heated at 105 °C for 0.5 h to inactivate enzymes, followed by drying at 80 °C to constant weight. The plant dry weight (PWD) was then recorded. PMC was calculated as PMC = (PWF − PWD)/PWF × 100%. Leaf moisture content (LMC). Leaves were sealed in bags to determine the leaf fresh weight (LWF). The samples were placed into pre-weighed kraft paper bags, enzyme-inactivated at 105 °C for 0.5 h, and dried at 80 °C to constant weight to obtain the leaf dry weight (LWD). LMC was calculated as LMC = (LWF − LWD)/LWF × 100%. Leaf equivalent water thickness (LEWT). Fresh leaves were weighed to obtain LWF and leaf area (A) was measured. Samples were then enzyme-inactivated at 105 °C for 1 h and dried at 75 °C to a constant weight to determine (LWD). LEWT was calculated as LEWT = (LWF − LWD)/(LWD × A) × 100%.

Biomass Measurements: Seedlings were sampled to determine the fresh weight of the above-ground parts (FWAG) and the underground parts (FUW). Samples were then enzyme inactivated at 105 °C, and subsequently dried at 80 °C to constant weight. The dry weights of the above-ground and below-ground (DUW) tissues were measured.

Antioxidant Enzyme Activities. Approximately 0.3 g of fresh leaf tissue was homogenized in 3 mL of prechilled 50 mM potassium phosphate buffer (pH 7.8) at 4 °C. The homogenate was centrifuged at 10,000× *g* for 20 min at 4 °C, and the supernatant was collected for enzyme activity assays. Activities of superoxide dismutase (SOD), peroxidase (POD), and catalase (CAT) were determined following established protocols [43]. Proline Content. Leaf tissue was homogenized in 3% (*w*/*v*) sulfosalicylic acid. After centrifugation, the supernatant was reacted with acidified ninhydrin reagent, and the absorbance of the resulting chromophore was measured at 520 nm using L-proline as the standard. Soluble Sugar Content. Samples were extracted with 80% (*v*/*v*) ethanol. The supernatant was mixed with 5% (*v*/*v*) phenol and concentrated sulfuric acid, and the absorbance of the developed color was measured at 490 nm. MDA content: Powdered leaf tissue was homogenized in 0.1% (*w*/*v*) thiobarbituric acid prepared in 10% (*w*/*v*) trichloroacetic acid. The mixture was heated at 95 °C for 30 min, cooled, and centrifuged. Absorbance of the supernatant was measured at 532 nm and 600 nm, and MDA concentration was calculated using an extinction coefficient of 155 $mM^{-1}cm^{-1}$. Soluble Protein Content. Protein concentration was determined using the Coomassie Brilliant Blue G-250 method with bovine serum albumin as the standard [44].

Phytohormone Analysis. Phytohormones were extracted, purified, and quantified using a previously established HPLC method. Approximately 1 g of frozen leaf powder, ground in liquid nitrogen, was homogenized in 8 mL of prechilled 80% (*v*/*v*) methanol and incubated in darkness at 4 °C for 12 h. The extract was then sonicated in the dark for 1 h, and centrifuged at 12,000× *g* for 15 min at 4 °C. The supernatant was transferred to a 10 mL tube, and 0.2 g of polyvinylpolypyrrolidone was added to remove phenolic compounds. The mixture was sonicated for 30 min and centrifuged again at 12,000× *g*, for 5 min at 4 °C. The resulting supernatant was, adjusted to pH 2.9 with glacial acetic acid, and purified using a C18 solid-phase extraction cartridge. Elution was performed with 1 mL of methanol (pH 8), and the eluate was collected in an HPLC vial for analysis. Reference standards for auxin (IAA), gibberellin (GA), zeatin (ZT), and ABA were used to construct calibration curves. Chromatographic separation was conducted on a Hitachi L-7420 HPLC system (Hitachi, Tokyo, Japan) using a mobile phase of methanol: 0.7% acetic acid: water (55:40:5, *v*/*v*/*v*) at a flow rate of 0.7 mL·min^{-1}. Detection was performed at 254 nm with the column temperature maintained at 30 °C and an injection volume of 10 µL [45].

Chlorophyll and Carotenoid Content. Chlorophyll a (Chl a), chlorophyll b (Chl b), total chlorophyll (Chl a + b), and carotenoid (Car) contents were determined using an acetone–ethanol mixed solvent extraction method [46]. Chlorophyll Fluorescence Parameters. Chlorophyll fluorescence was measured with a compact multi-channel monitoring fluorometer (Miro-PAM) (Zealquest Scientific Technology, Shanghai, China) employing pulse-amplitude modulation (PAM) technology. Measured parameters included minimal fluorescence (F_0), maximal fluorescence (Fm), maximum quantum efficiency of PSII photochemistry (Fv/Fm), electron transport rate, photochemical quenching (qP), non-photochemical quenching (NPQ), and the quantum yield of non-photochemical quenching (qN) [47].

2.4. Transcriptome Analysis Under Drought Stress

Transcriptome Analysis. Leaf samples corresponding to those used for physiological measurements were selected for transcriptome profiling. Total RNA was extracted from leaf tissues under control and drought-stress conditions using TRIzol reagent (Invitrogen, Waltham, MA, USA), according to the manufacturer's instructions. Each RNA sample represented a pooled mixture of five individual plants, with three biological replicates per treatment. After verifying RNA quality, sequencing libraries were constructed through cDNA synthesis and purification. Library sequencing was performed on an Illumina HiSeq platform (Illumina, San Diego, CA, USA). Raw sequencing data underwent quality control to remove adapter sequences, low-quality reads, and poly-N sequences, yielding high-quality clean reads. Clean reads were aligned to the cabbage reference genome (GCF_000695525.1) using HISAT2. Then differentially expressed genes (DEGs) were analyzed by DESeq (v1.22.1) with screened conditions as follows: different expression multiple $|\log2FoldChange| > 1$, an adjusted *p*-value (padj) < 0.05. Gene Ontology (GO) and KEGG pathway enrichment analyses of DEGs were conducted using ShinyGO v0.75, with FDR < 0.05 considered statistically significant.

2.5. Metabolomic Analysis Under Drought Stress

Metabolomic Profiling. For metabolomic analysis under drought stress, leaf samples from each treatment group were collected with six biological replicates. Leaf tissues were ground into a homogeneous powder, and 400 mg of each replicate was accurately weighed. Subsequently, 2 mL of methanol was added, and the mixture was vortexed for 10 s, followed by ultrasonic extraction at 70 °C. After centrifugation at 12,000× *g*, the supernatant was collected. Then, 2 mL of ultrapure water and 1 mL of chloroform were added, followed by centrifugation at 14,000× *g* for 5 min. A 400 µL aliquot of the supernatant was transferred to a sample vial and dried under nitrogen gas. The residue was reconstituted in 80 µL of methoxyamine pyridine solution (15 mg mL^{-1}), vortexed for 30 s, and incubated at 37 °C for 90 min. Subsequently, 80 µL of BSTFA (with 1% TMCS) was added, and the mixture was derivatized at 70 °C for 60 min before LC-MS analysis.

LC-MS Analysis. Metabolite separation was performed using an Agilent 6890 LC system coupled with an HP-5MS capillary column (30 m × 0.25 mm, 0.25 µm film thickness). The injector temperature was set to 250 °C. The oven temperature program was initial temperature 80 °C held for 3 min, ramped to 280 °C at 10 °C min^{-1}, and held for 2 min. High-purity helium was used as the carrier gas at a constant flow rate of 1.0 $mLmin^{-1}$. Samples were injected in splitless mode with a 1 µL injection volume of 1 µL. Detection was carried out using an Agilent 5973 mass spectrometer (Agilent Technologies, Santa Clara, CA, USA) with the ion source temperature set to 230 °C and the quadrupole temperature set to 150 °C. The mass scanning range was 50–800 m/z with a mass accuracy of 0.1 amu and ionization was initiated after a 180 s solvent delay.

2.6. Combined Transcriptomic and Metabolome Analysis

Pathways simultaneously enriched with both DEGs and differentially accumulated metabolites under each treatment condition were identified. The resulting co-enriched pathways were visualized using through KEGG pathway mapping.

2.7. Data Analysis

Data Analysis. Statistical analyses were performed using SPSS 22.0 (IBM, Armonk, NY, USA), including one-way analysis of variance and Duncan's multiple range test, with significance set at $p < 0.05$. All data are presented as means ± standard deviation of three biological replicates. Cluster heatmaps were generated using an online tool (https://cloud.metware.cn (accessed on 20 December 2025)). Principal component analysis and orthogonal partial least squares-discriminant analysis were conducted using an online platform (https://www.omicshare.com/tools (accessed on 20 December 2025)). Correlation analysis for all 24 sample groups was performed using the BMK Cloud platform (https://international.biocloud.net (accessed on 25 December 2025)). All figures were prepared with Origin 2021 (Origin Lab, Northampton, MA, USA).

3. Results

3.1. Screening of Drought-Tolerant and Drought-Sensitive Cabbage Genotypes

The seed germination rate and the germination drought resistance index are key parameters for evaluating drought tolerance during the seed germination stage. This study employed 29 cabbage varieties as experimental materials. Drought stress was simulated using a 20% PEG-6000 solution to evaluate seed germination characteristics systematically. Comparative analysis of germination performance identified two lines with distinct phenotypic differences (Figure 1A–C). Among these, 'ZG-628' demonstrated the highest relative germination rate (96.55%) and germination drought resistance index (1.00), whereas 'ZG-21' showed the lowest values for both parameters (0.00% and 0.00). Consequently, 'ZG-628' was categorized as drought-tolerant and 'ZG-21' as drought-sensitive, establishing them as key candidates for subsequent investigation into the drought tolerance mechanisms of cabbage.

To further evaluate the drought resistance of these selected lines at the seedling stage, plants were subjected to varying intensities of water deficit. The substrate relative water content was used as the stress metric, with 80% representing the well-watered control and 40% representing severe drought (Figure 1D). Under well-watered conditions, both 'ZG-628' and 'ZG-21' displayed normal phenotypes without visible abnormalities. In contrast, growth inhibition was more evident in 'ZG-21' than in 'ZG-628'.

3.2. Effects of Drought Stress on Physiological Characteristics of Cabbage Leaves

Under drought stress, various physiological indicators were measured for the two varieties. To quantify their differences in tolerance to drought-induced damage, water status parameters and biomass were determined. The results showed that the drought-induced reduction in plant moisture content (PMC) was smaller in 'ZG-628' (7.0%) than in 'ZG-21' (11.0%) (Figure 2A). The leaf moisture content (LMC) was higher in 'ZG-628' (91.28%) compared to 'ZG-21' (84.90%), indicating better maintenance of water status in the former. Similarly, the leaf equivalent water thickness (EWT) was greater in 'ZG-628' (0.0030) than in 'ZG-21' (0.0027), suggesting enhanced internal water storage in its leaf tissues. Furthermore, all measured biomass parameters, including shoot fresh weight (1.69), shoot dry weight (0.1023), root fresh weight (0.1087), and root dry weight (0.0202) were consistently higher in 'ZG-628' than the corresponding values in 'ZG-21' (shoot fresh weight: 0.72; shoot dry weight: 0.0645; root fresh weight: 0.0791; root dry weight: 0.0113). These findings

collectively demonstrate that the drought-tolerant 'ZG-628' maintains better water status and biomass accumulation under drought stress relative to the drought-sensitive 'ZG-21'.

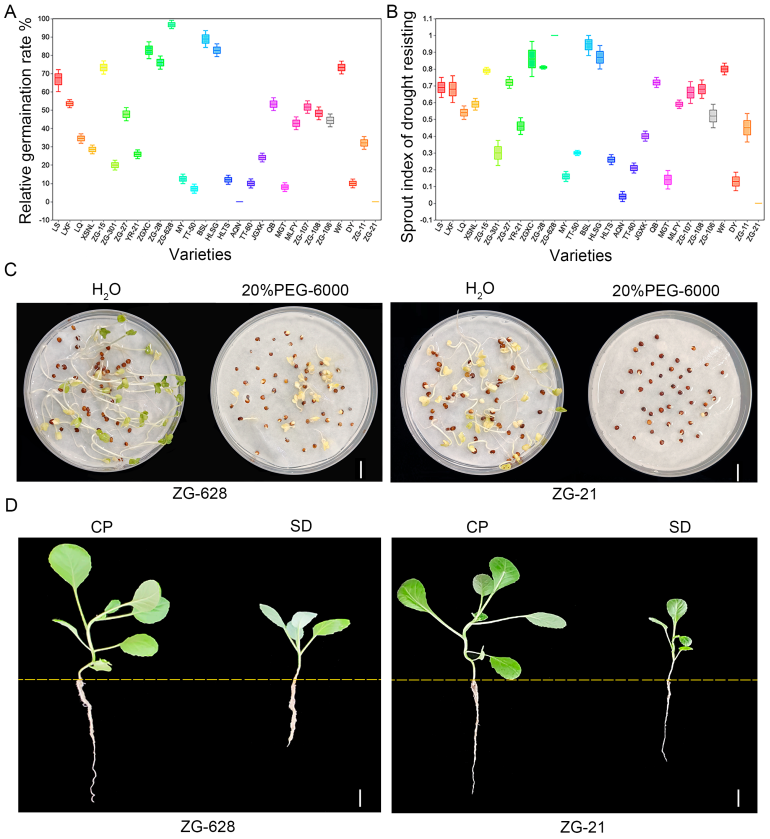


Figure 1. Effects of drought stress on seed germination and seedling growth. (**A**) Box plot of relative germination efficiency (RGE) for 29 cabbage varieties. (**B**) Box plot of germination drought resistance index (GDRI) for 29 cabbage varieties. (**C**) Seed germination performance of ZG-628 and ZG-21 under H_2O and 20% PEG-6000 simulated drought stress. (**D**) Seedling growth performance of ZG-628 and ZG-21 under adequate H_2O (CP) and severe drought stress (SD) conditions. Note: The yellow dashed line indicates the soil surface, separating the aboveground and belowground portions of the plants. Scale bar = 2 cm.

To elucidate the physiological mechanisms underlying drought tolerance, we assessed leaf antioxidant enzyme activities and osmoregulatory substance contents in the two cabbage varieties under drought stress. The activities of key antioxidant enzymes, superoxide dismutase (SOD), peroxidase (POD), and catalase (CAT) were higher in 'ZG-628' (534.69 U/g FW, 1706.67 U/g FW, and 208.00 U/g FW, respectively) than those in 'ZG-21' (208.50 U/g FW, 1350.00 U/g FW, and 150.67 U/g FW) (Figure 2B). This indicates a more efficient reactive oxygen species (ROS) scavenging capacity in the drought-tolerant line. Correspondingly, the malondialdehyde (MDA) content was markedly lower in 'ZG-628' (2.27 μmol/g FW) than in 'ZG-21' (4.54 μmol/g FW), suggesting reduced membrane lipid peroxidation and enhanced cellular membrane integrity. Furthermore, 'ZG-628' accumulated higher levels of osmoregulatory substances, with proline at 85.38 μg/g compared to 68.48 μg/g in 'ZG-21', soluble protein at 9.34 mg/g versus 7.18 mg/g in 'ZG-21', and soluble sugar at 1.35 mg/g relative to 0.87 mg/g in 'ZG-21'. These results collectively highlight a stronger osmotic adjustment capacity in 'ZG-628', which contributes to the maintenance of cellular water balance. In summary, the enhanced drought tolerance of 'ZG-628' is attributed to a coordinated physiological strategy involving elevated antioxidant enzyme activities and increased accumulation of osmoregulatory solutes, thereby alleviating oxidative damage and cellular dehydration under stress conditions.

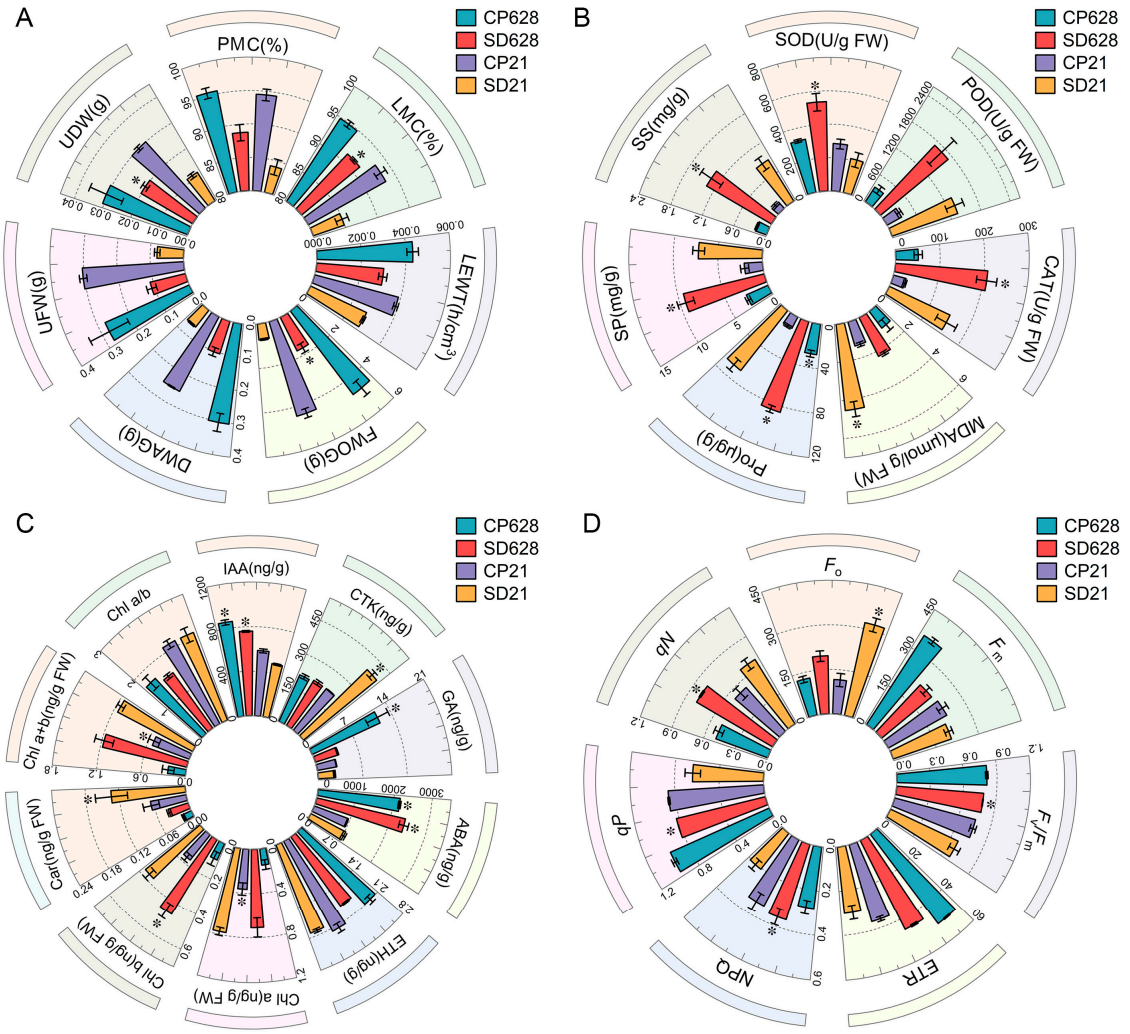


Figure 2. Effects of drought stress on physiological and biochemical indicators during the seedling stage of cabbage. (**A**) Changes in water status parameters and biomass. (**B**) Changes in antioxidant enzyme activities and osmotic regulator content. (**C**) Changes in hormone and photosynthetic pigment content. (**D**) Changes in chlorophyll fluorescence parameters. Note: PMC, plant moisture content; LMC, leaf moisture content; LEWT, leaf equivalent water thickness; FWOG, fresh weight of aboveground parts; DWAG, dry weight of aboveground parts; UFW, fresh weight of belowground parts; UDW, dry weight of belowground parts. SOD: Superoxide Dismutase; POD: Peroxidase; CAT: Catalase; MDA: Malondialdehyde; Pro: Proline; SP: Soluble Protein; SS: Soluble Sugar. ABA: Abscisic Acid. IAA: Indole-3-Acetic Acid. GA: Gibberellin. CTK: Cytokinin. Chl a: Chlorophyll a. Chl b: Chlorophyll b. Car: Carotenoids. Chl a + Chl b: Total Chlorophyll. Chl a/Chl b: Chlorophyll a/Chlorophyll b ratio. Fo: F minimal fluorescence. Fm: F maximal fluorescence. Fv/Fm: F variable/F maximal ratio. ETR: Electron Transport Rate. NPQ: Non-Photochemical Quenching. qP: Photochemical quenching coefficient. qN: Non-photochemical quenching coefficient. The data were analyzed using one-way analysis of variance (ANOVA) in SPSS 22.0 software (IBM, Armonk, NY, USA), and the significance of differences among treatment means was assessed using Duncan's test ($p < 0.05$). Data are presented as mean ± SD of three biological replicates, where * indicates a significant difference compared with the Control group.

The results demonstrated that drought stress altered the contents of endogenous hormones and photosynthetic pigments in both cabbage varieties. Regarding hormonal responses (Figure 2C), the ABA content in 'ZG-628' under drought stress reached 2388.57 ng/g, exceeding that in 'ZG-21' (1030.67 ng/g), which suggests more pronounced stress signaling activation in the drought-tolerant variety. The contents of auxin (IAA) and

gibberellin (GA) in 'ZG-628' under drought were 758.60 ng/g and 3.77 ng/g, respectively. Although these values represented a decrease compared to its well-watered control, they remained higher than those in drought-stressed 'ZG-21' (IAA: 482.34 ng/g; GA: 2.59 ng/g), indicating a relatively stronger potential for growth maintenance under stress. In contrast, the cytokinin (CTK) content in 'ZG-21' increased to 389.78 ng/g under drought, which may reflect a distinct regulatory strategy. With respect to photosynthetic pigments (Figure 2C), 'ZG-628' under drought maintained higher levels of chlorophyll a (0.71 mg/g), chlorophyll b (0.46 mg/g), and total chlorophyll (Chl a + b: 1.17 mg/g) than its control, with chlorophyll b content being higher than that in 'ZG-21' (0.37 mg/g). This indicates a superior capacity for photosynthetic apparatus preservation under stress. In summary, the drought-tolerant 'ZG-628' appears to achieve an optimized balance between stress response and photosynthetic maintenance through enhanced ABA-mediated signaling and sustained accumulation of key photosynthetic pigments.

To characterize the photosynthetic responses to drought stress, chlorophyll fluorescence parameters were systematically evaluated in the two cabbage varieties. Under drought conditions, the initial fluorescence (Fo) was lower in 'ZG-628' (195.6) than in 'ZG-21' (319.7), indicating less impairment of the PSII reaction centers in the drought-tolerant line (Figure 2D). Concurrently, 'ZG-628' exhibited a higher maximum fluorescence (Fm) (218.1) compared to 'ZG-21' (207.4), suggesting better preservation of PSII photochemical potential. The maximum photochemical efficiency of PSII (Fv/Fm) was also higher in 'ZG-628' (0.784) than in 'ZG-21' (0.671), reflecting its superior capacity for light energy conversion under stress. With respect to electron transport, the electron transport rate (ETR) was markedly elevated in 'ZG-628' (44.98) relative to 'ZG-21' (30.14), indicating more robust photosynthetic electron flow. In addition, non-photochemical quenching (NPQ) was enhanced in 'ZG-628' (0.357) compared to 'ZG-21' (0.205), demonstrating a more effective dissipation of excess excitation energy as heat. The photochemical quenching coefficient (qP) was also higher in 'ZG-628' (0.823) than in 'ZG-21' (0.637), further supporting a greater proportion of open PSII reaction centers and sustained electron transport capacity. Collectively, these results illustrate that 'ZG-628' maintains higher photosynthetic performance under drought through coordinated improvements in energy capture, electron transport, and photoprotective dissipation.

3.3. Comparative Transcriptome Analysis of "ZG-628" and "ZG-21" in Response to Drought

Beyond physiological adaptations, drought stress also induced substantial changes in the transcriptomic profiles of cabbage. To systematically characterize the expression patterns and functional attributes of DEGs, we performed RNA sequencing on 12 samples representing four experimental groups, CP628, SD628, CP21, and SD21, each with three biological replicates. After rigorous quality control, including filtering based on sequencing error rate and GC content distribution, a total of 79.03 GB of clean data were obtained. Each sample contributed no less than 6.16 Gb of clean data, with Q30 scores all above 90.1% (Table S1). The clean reads were subsequently aligned to the reference genome, yielding alignment rates between 84.28% and 87.1%, confirming the high quality and suitability of the data for downstream analysis. Functional annotation was carried out using multiple databases, including GO, KEGG, EggNOG, NR, Swiss-Prot, and Pfam. The annotation results were as follows: 32,588 genes were annotated in GO, 16,402 in KEGG, 37,888 in EggNOG, 41,202 in NR, 32,843 in Swiss-Prot, and 30,651 in Pfam (Table S2). To clarify the overall transcriptional differences among treatments, principal component analysis (PCA) was performed on samples from the four treatment groups: CP21, CP628, SD21, and SD628. The results revealed distinct clustering of samples from each group in the principal component space. CP628 and SD628 were positioned closer to each other, while

CP21 and SD21 formed separate clusters. Notably, CP21 exhibited the most pronounced transcriptional divergence from all other groups (Figure S1).

KEGG pathway enrichment analysis results are summarized in the bubble plot presented in Figure 3. Enrichment significance was evaluated using the Rich factor (the ratio of enriched genes to annotated genes in a pathway, with higher values indicating greater enrichment), the adjusted *p*-value (Padjust, with lower values representing stronger statistical significance), and the number of genes assigned to each pathway. The DEGs were enriched in several key pathways, including ribosome, flavonoid biosynthesis, oxidative phosphorylation, spliceosome, plant hormone signal transduction, MAPK signaling pathway–plant, cysteine and methionine metabolism, peroxisome, ABC transporters, and glycerophospholipid metabolism. In parallel, GO enrichment analysis indicated that the DEGs were primarily involved in biological processes and molecular functions such as SSU-rRNA maturation, protein autophosphorylation, orotate phosphoribosyltransferase activity, and the de novo UMP biosynthetic process (Figure S1). Additionally, KEGG-based categorical annotation revealed that the DEGs were predominantly associated with four major functional categories: metabolism, genetic information processing, cellular processes, and organismal systems (Figure S2).

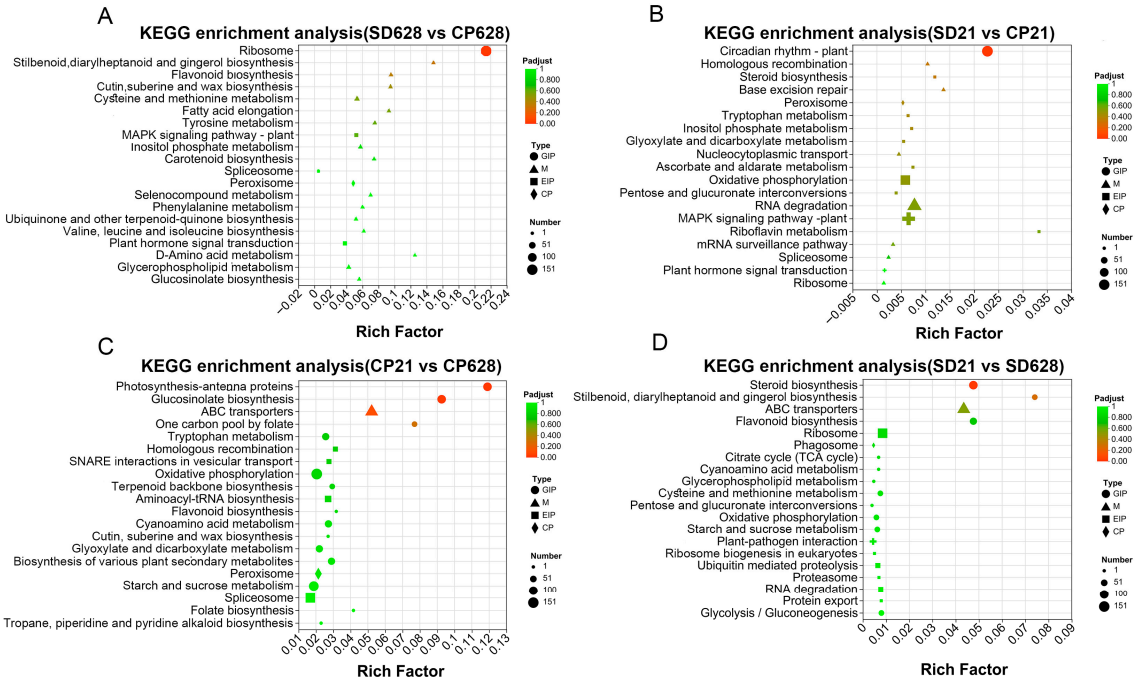


Figure 3. KEGG enrichment analysis of differentially expressed genes after drought stress treatment. (**A**) KEGG enrichment analysis of DEGs in ZG-628 under drought stress (SD628) compared to control conditions (CP628). (**B**) KEGG enrichment analysis of DEGs in ZG-21 under drought stress (SD21) compared to control conditions (CP21). (**C**) KEGG enrichment analysis of DEGs in ZG-21 (CP21) compared to ZG-628 (CP628) under control conditions. (**D**) KEGG enrichment analysis of DEGs in ZG-21 (SD21) compared to ZG-628 (SD628) under drought stress conditions. Note: The color of each node represents the *p*-value, while its size indicates the number of differentially expressed genes. The enrichment factor (Rich factor) reflects the degree of enrichment. Colors transition from red to green, indicating progressively lower *p*-values. Larger nodes denote greater gene enrichment within that pathway. Higher enrichment factors signify stronger enrichment levels. In the figure, distinct shapes denote different categories of metabolic pathways: circles represent Genetic Information Processing, triangles represent Metabolism, rectangles represent Environmental Information Processing, and diamonds represent Cellular Processes.

DEGs were identified using DESeq2, with thresholds set at $|\log_2 (\text{fold change})| > 1$ and a false discovery rate (FDR) < 0.05. Under control conditions, comparison between the two varieties (CP21 vs. CP628) revealed 676 DEGs, comprising 371 up-regulated and 305 down-regulated genes (Figure 4A). Under severe drought stress, the inter-varietal comparison (SD21 vs. SD628) identified 623 DEGs (338 up-regulated and 285 down-regulated), indicating that drought stress accentuated transcriptomic divergence between the drought-tolerant and drought-sensitive varieties. From an intra-varietal perspective, drought stress triggered 75 DEGs (54 up-regulated and 21 down-regulated) in the sensitive variety 'ZG-21' (SD21 vs. CP21), whereas it induced 1362 DEGs (772 up-regulated and 590 down-regulated) in the tolerant variety 'ZG-628' (SD628 vs. CP628). The substantially greater number of drought-responsive DEGs in 'ZG-628' suggests a more extensive transcriptional reprogramming upon drought imposition. A Venn diagram illustrated the overlap of DEGs among the four comparison groups (Figure 4B), with one common DEG shared across all sets. Group-specific DEGs included 247 unique to SD21 vs. SD628, 54 to SD21 vs. CP21, 340 to CP21 vs. CP628, and 1290 to SD628 vs. CP628.

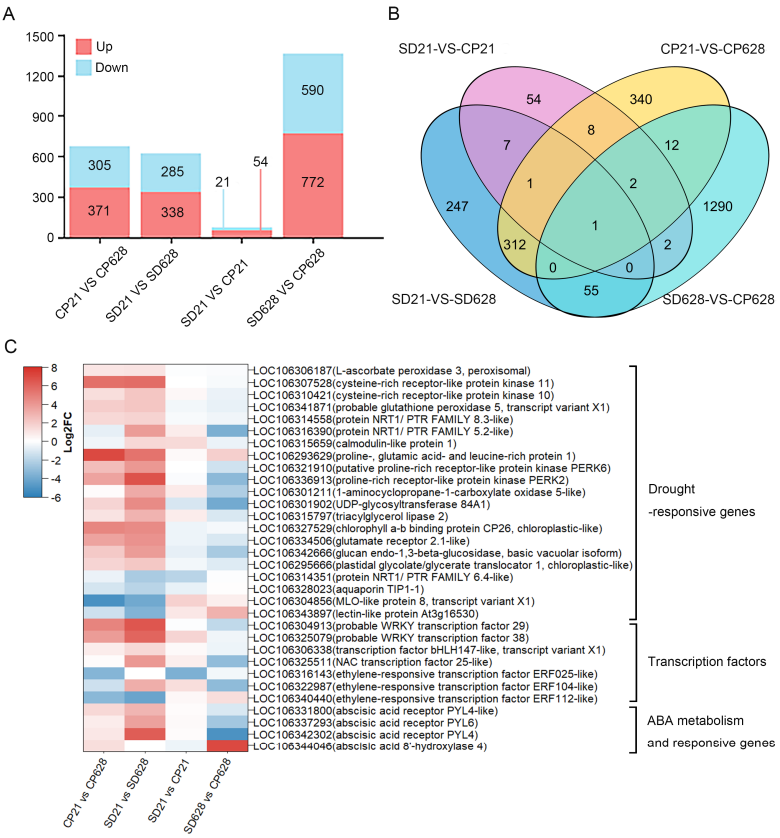


Figure 4. Transcriptome Analysis of DEGs Under Drought Stress. (**A**) statistical data of DEGs in the (CP21 vs. CP628), (SD21 vs. SD628), (SD21 vs. CP21), (SD628 vs. CP628) comparisons. (**B**) Veen diagram of DEGs in the CP21 vs. CP628), (SD21 vs. SD628), (SD21 vs. CP21), (SD628 vs. CP628) comparisons. The numbers represent the total numbers of DEGs in different comparison groups. (**C**) Hierarchical clustering of drought-responsive genes among the DEGs. Note: The heatmap shows fold changes in the abundance of gene transcripts in different comparison groups.

To delineate the core molecular regulatory mechanisms underlying differential drought responses between 'ZG-628' and 'ZG-21', we performed hierarchical clustering analysis on selected DEGs under drought stress (Figure 4C). Relative to the control comparison (CP21 vs. CP628), most stress-responsive genes, particularly those associated with ROS scavenging, signal transduction, and osmoregulation, were upregulated in the variety-to-variety drought comparison (SD21 vs. SD628). By contrast, the same set of genes were

either downregulated or remained unchanged in the self-comparison under drought in the tolerant line (SD628 vs. CP628). Representative genes exhibiting this pattern included those encoding a proline-, glutamic acid- and leucine-rich protein (*LOC106293629*), a cysteine-rich receptor-like protein kinase (*LOC106307528*), a WRKY transcription factor (LOC106304913), and a chlorophyll a-b binding protein (*LOC106327529*). Notably, several genes displayed opposing expression trends between the two drought-related comparisons. For instance, aquaporin TIP1 (*LOC106328023*), MLO-like protein (LOC106304856), and lectin-like protein (*LOC106343897*) were downregulated in SD21 vs. SD628 but upregulated in SD628 vs. CP628. Beyond classical stress-responsive genes, multiple transcription factors, including WRKY (*LOC106304913*, *LOC106325079*), bHLH147-like (*LOC106306338*), and NAC (*LOC106325511*), were upregulated in SD21 vs. SD628 yet downregulated in SD628 vs. CP628. Concurrently, ABA-responsive gene expression was markedly enhanced. All annotated abscisic acid receptor genes (*LOC106331800*, *LOC106337293*, *LOC106342302*) were upregulated in SD21 vs. SD628 but downregulated in SD628 vs. CP628.

3.4. Comparative Metabolome Analysis of "ZG-628" and "ZG-21" in Response to Drought

Comprehensive metabolomic profiling of heading cabbage leaves identified 534 secondary metabolites, which were categorized into 12 distinct classes (Figure 5A). These include terpenoids, phenolic acids and derivatives, flavonoids, steroids and steroid derivatives, organic acids and derivatives, indoles and derivatives, coumarins and derivatives, alkaloids and derivatives, stilbenes, quinones, lignans and derivatives, and tannins. Terpenoids constituted the most abundant category with 191 metabolites, followed by phenolic acids and derivatives (68) and flavonoids (65). Hierarchical clustering analysis demonstrated clear separation between full irrigation and severe drought stress groups in both varieties, with samples clustering consistently by genotype, indicating that drought stress reshapes the leaf metabolome (Figure 5B).

To systematically uncover key metabolites involved in drought stress response in cabbage, we conducted Orthogonal Partial Least Squares-Discriminant Analysis (OPLS-DDA) on varieties 628 and 21 under both control and drought conditions. The established OPLS-DA models explained 22.20% and 21.30% of the total metabolic variance in varieties 628 and 21, respectively (Figure 5C–F). Comparative profiling between severe drought (SD628) and well-watered (CP628) treatments in variety 628 uncovered 340 DAMs (Figure 5G), whereas 306 were identified in the corresponding comparison in variety 21 (SD21 vs. CP21). Further analysis revealed 222 DAMs between the two varieties under drought (SD21 vs. SD628), and 276 under control conditions (CP21 vs. CP628). Notably, nine common DAMs were identified across all four treatment groups of the two genotypes under drought conditions.

Based on a variable importance in projection (VIP) threshold > 1, 340 and 306 metabolites were identified as drought-responsive in varieties 628 and 21, respectively (Tables S4 and S5). Intersection analysis revealed 198 metabolites common to both genotypes under drought stress (Figure 6C). The top 50 drought-responsive metabolites in each variety, along with their accumulation patterns, are displayed in Figure 6A,B. Among these, 29 metabolites were shared between the two genotypes, including known drought-associated compounds such as abscisic acid and 2-keto-6-acetamidocaproate. Additionally, several flavonoid metabolites, including isorhamnetin 3-rutinoside 4′-rhamnoside, luteolin, quercetin 3-sophorotrioside 7-rhamnoside, and quercetin 3-rutinoside 3′,7-diglucoside, were specifically identified as drought-responsive only in variety 628.

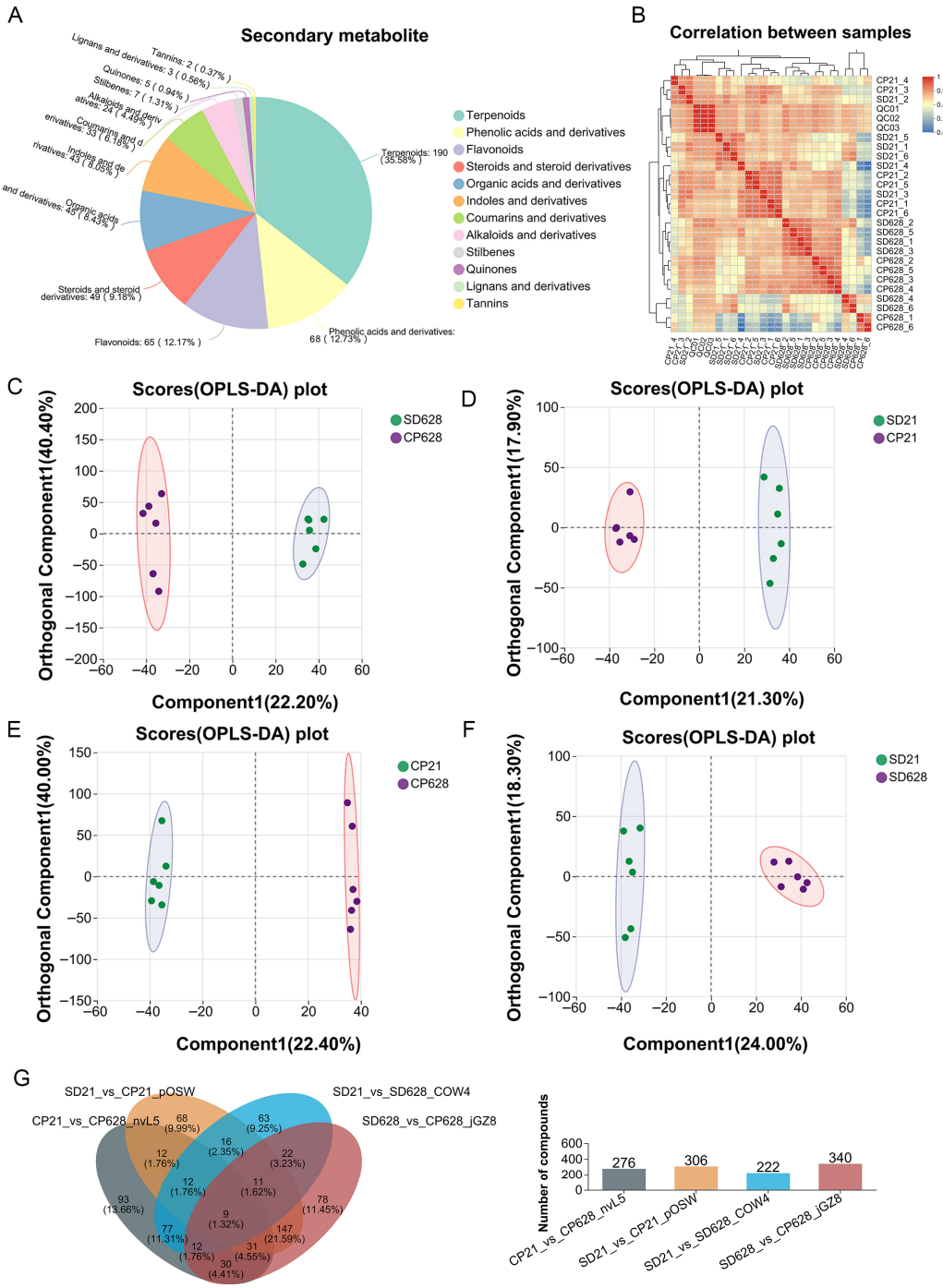


Figure 5. Analysis of DAMs under drought stress. (**A**) Metabolite categories. (**B**) Hierarchical clustering heatmap of metabolites across all samples. (**C**) OPLS-DA score plot for SD628 vs. CP628. (**D**) OPLS-DA score plot for SD21 vs. CP21. (**E**) OPLS-DA score plot for CP21 vs. CP628. (**F**) OPLS-DA score plot for SD21 vs. SD628. (**G**) Venn diagram of DAMs in the four comparison groups and bar chart showing the number of DAMs in each comparison. Note: The *** symbols denote genes with a statistically significant difference in expression at a threshold of $p < 0.001$.

KEGG pathway enrichment analysis of DAMs identified nine pathways shared between the SD628 vs. CP628 and SD21 vs. CP21 comparisons. Among these, "Alpha-linolenic acid metabolism," "Nucleotide metabolism," and "Purine metabolism" showed the most significant enrichment (Figure 7A,B). Additionally, eleven pathways were commonly enriched in both the CP21 vs. CP628 and SD21 vs. SD628 comparisons, with "Tryptophan metabolism," "Pantothenate and CoA biosynthesis," and "beta-Alanine metabolism"

exhibiting the most marked enrichment (Figure 7C,D). Compared to the SD21 vs. CP21 comparison (Figure 7B), three pathways were uniquely and enriched in the SD628 vs. CP628 comparison (Figure 7A): "Tyrosine metabolism," "Flavonoid and flavonol biosynthesis," and "Pyrimidine metabolism." These pathways may contribute specifically to drought tolerance in heading cabbage. Notably, three pathways, "Linoleic acid metabolism," "Pantothenate and CoA biosynthesis," and "beta-Alanine metabolism", were consistently enriched across all four comparisons: SD628 vs. CP628, SD21 vs. CP21, CP21 vs. CP628, and SD21 vs. SD628.

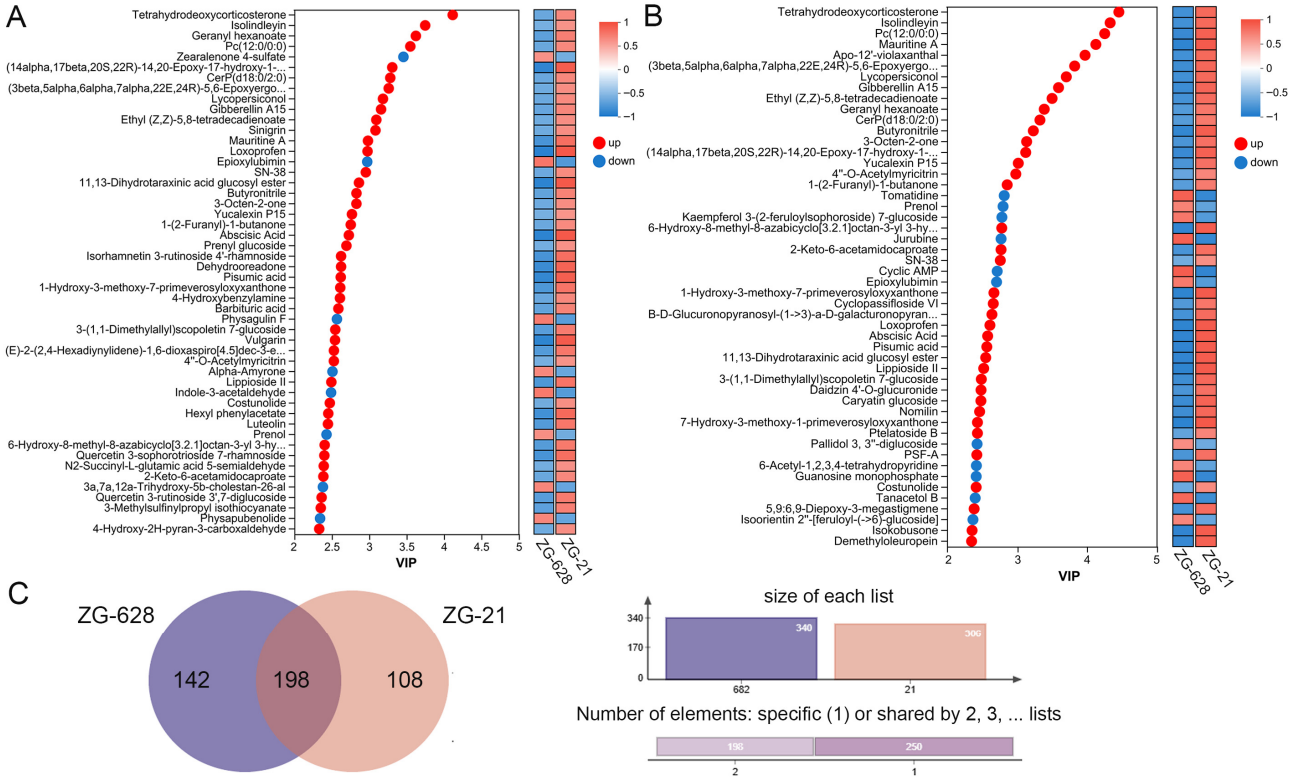


Figure 6. Important metabolites in response to drought stress identified by partial least squares-discriminant analysis (PLS-DA) in ZG-628 and ZG-21. (**A**,**B**) Fifty top metabolites according to the VIP (variable importance in projection) score in drought-tolerant (ZG-628) and drought-sensitive (ZG-21) cabbage are shown. (**C**) Overlap among drought-responsive metabolites in ZG-628 and ZG-21.

K-means clustering analysis was applied to characterize the dynamic accumulation profiles of metabolites in heading cabbage leaves across different treatment conditions (Figure 7E–H). Clusters 1 and 4 contained the highest number of metabolites, comprising 359 and 353 compounds, respectively. Metabolites in Cluster 1 peaked in the SD628 treatment group, whereas those in Cluster 3 reached their highest levels in CP628 but showed relatively lower accumulation under SD628 conditions. Cluster 4 metabolites were predominantly accumulated in both CP21 and SD21 groups. Conversely, Cluster 2 displayed elevated metabolite accumulation in CP628 and SD628. Notably, several metabolites in Cluster 2, including 2,3-Dihydroabscisic alcohol and Abscisic alcohol, are associated with the ABA metabolic pathway.

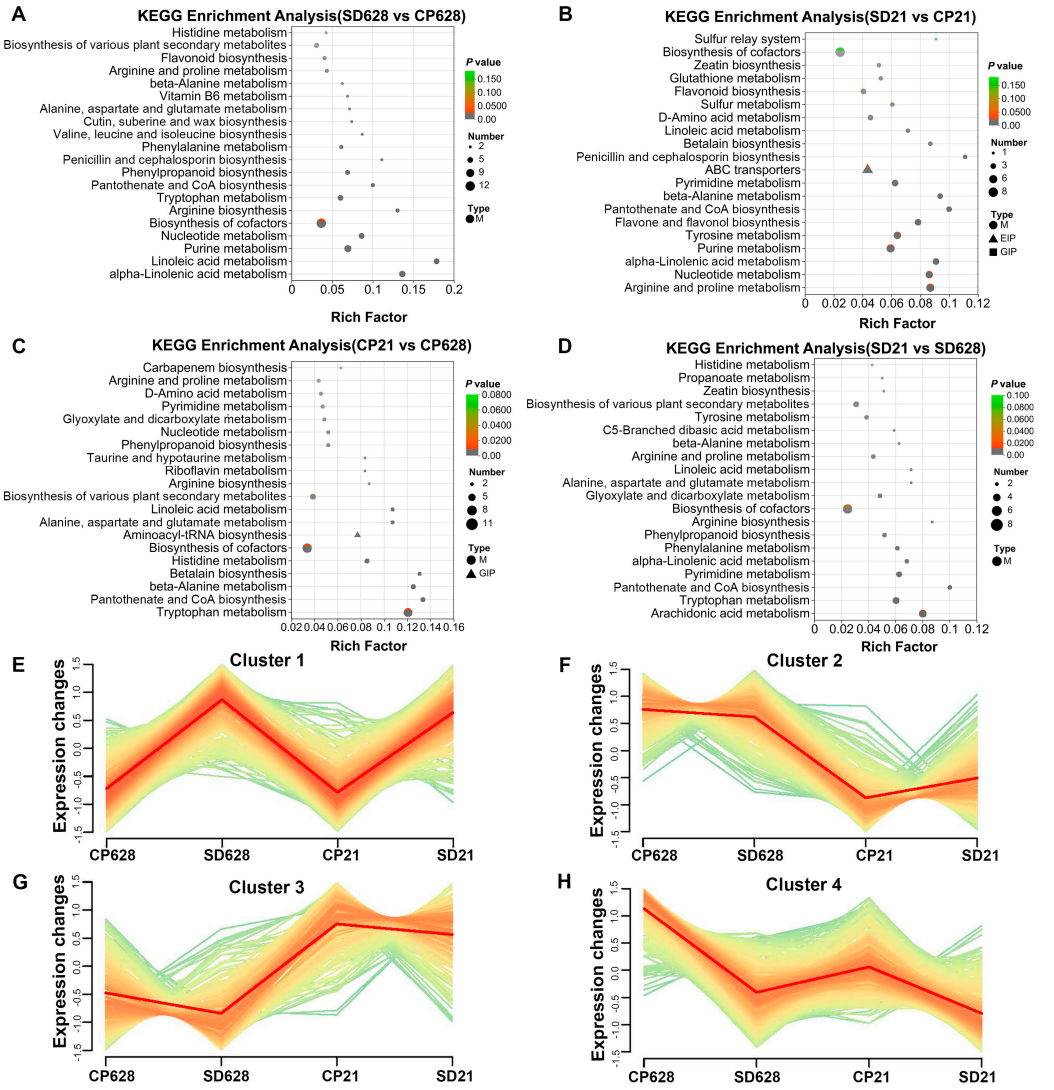


Figure 7. KEGG enrichment analysis and K-means clustering analysis of metabolites under drought stress. (**A**–**D**) KEGG enrichment analysis of metabolites across four comparison groups. (**E**–**H**) K-means clustering analysis of metabolites across four comparison groups. Note: In the figure, distinct shapes denote different categories of metabolic pathways: circles represent Genetic Information Processing, triangles represent Metabolism, rectangles represent Environmental Information Processing.

3.5. Integrated Analysis of Differentially Expressed Genes and Differentially Accumulated Metabolites Responding to Drought Stress

Integrated KEGG pathway enrichment analysis of transcriptomic and metabolomic data revealed pronounced and dynamic genotypic differences between the two cabbage varieties, 'ZG-628' and 'ZG-21', in both basal metabolism and drought-responsive pathways. Under well-watered conditions (CP21 vs. CP628), pathways related to photosynthesis, glucosinolate biosynthesis, ABC transporters, and amino acid metabolism were already significantly enriched between the two varieties, indicating inherent genetic differences in their basal metabolic and transport mechanisms (Figure 8A). Under drought stress conditions (SD21 vs. SD628), metabolomic analysis showed significant enrichment in pathways such as flavonoid biosynthesis, phenylpropanoid biosynthesis, and alpha-linolenic acid metabolism (Figure 8B). In parallel, transcriptomic data revealed enrichment in key regulatory pathways including plant hormone signal transduction. The co-enrichment of flavonoid and phenylpropanoid biosynthesis pathways across both omics layers highlights coordinated regulation between gene expression and metabolite accumulation in

response to drought. Drought stress significantly reshaped both the transcriptome and metabolome of cabbage leaves (Figure S3). Spearman correlation analysis between DEGs and DAMs revealed that under well-watered conditions, metabolite-gene associations were weak but detectable in pathways such as photosynthesis and glucosinolate biosynthesis. Under drought, flavonoids, phenylpropanoids, and amino acid metabolites correlated strongly ($p < 0.05$) with genes in hormone signaling, secondary metabolism, and stress responses, forming a complex, bidirectional regulatory network. Statistical analysis of pathway-associated alterations in genes and metabolites was performed using the KEGG database. The top 20 pathways with the highest combined significance from both genomic and metabolomic annotations were selected for analysis in each dataset (Figure 8C,D). A total of 57 metabolic pathways were annotated across both 'ZG-628' and 'ZG-21', with 19 pathways shared between the two varieties, 18 unique to 'ZG-628', and 20 unique to 'ZG-21'. Pathways uniquely identified in 'ZG-628' included Cutin, suberine and wax biosynthesis, Starch and sucrose metabolism, Phenylpropanoid biosynthesis, Phenylalanine metabolism, and Arginine biosynthesis. KEGG pathways concurrently annotated in both transcriptomic and metabolomic datasets were subsequently identified for 'ZG-628' and 'ZG-21' (Figure S3). Three pathways were common to both varieties: Plant hormone signal transduction, Tryptophan metabolism, and Riboflavin metabolism. Notably, 42 pathways were unique to 'ZG-628', primarily including Glycolysis/Gluconeogenesis, Glutathione metabolism, Arginine and proline metabolism, Flavonoid biosynthesis, and Cutin, suberine and wax biosynthesis. Integrated analysis revealed that among the pathways co-annotated in both omics datasets under drought stress, Plant hormone signal transduction contained the highest number of DEGs. These findings demonstrate substantial differences in drought response mechanisms between the two cabbage varieties, with respiratory metabolism and plant hormone signal transduction playing particularly crucial roles in drought stress adaptation.

The drought-tolerant cabbage cultivar 'ZG-628' employs a multi-faceted strategy to cope with water deficit, sustaining photosynthetic performance, preserving hydraulic status, enhancing antioxidative capacity, regulating osmotic homeostasis, and modulating hormonal signaling (Figure 9). These coordinated physiological responses are closely linked to its efficient ABA-mediated regulatory network. Under drought conditions, elevated ABA levels are perceived by specific ABA receptors, including PYL4, PYL4-like, and PYL6. ABA binding suppresses the activity of type 2C protein phosphatases (PP2Cs), thereby releasing sucrose non-fermenting-related protein kinase 2s (SnRK2s) from inhibition. The activated SnRK2s in turn phosphorylate downstream transcription factors such as WRKY29, WRKY38, and NAC25-like, initiating the expression of drought-responsive genes. Concurrently, ABA perception by NRT1.1/PTR4 (Nitrate Transporter 1.1/Peptide Transporter 4) promotes its interaction with the cytosolic repressor SPX4. Under well-watered conditions, SPX4 sequesters the transcription factor NLP4 in the cytosol, preventing its nuclear translocation. Under drought stress, however, ABA enhances the NRT–SPX4 interaction, leading to the release of NLP4, which subsequently translocates into the nucleus. As a key transcriptional regulator in ABA signaling, nuclear-localized NLP4 directly binds to and activates a suite of ABA-responsive genes, further amplifying the drought adaptive response.

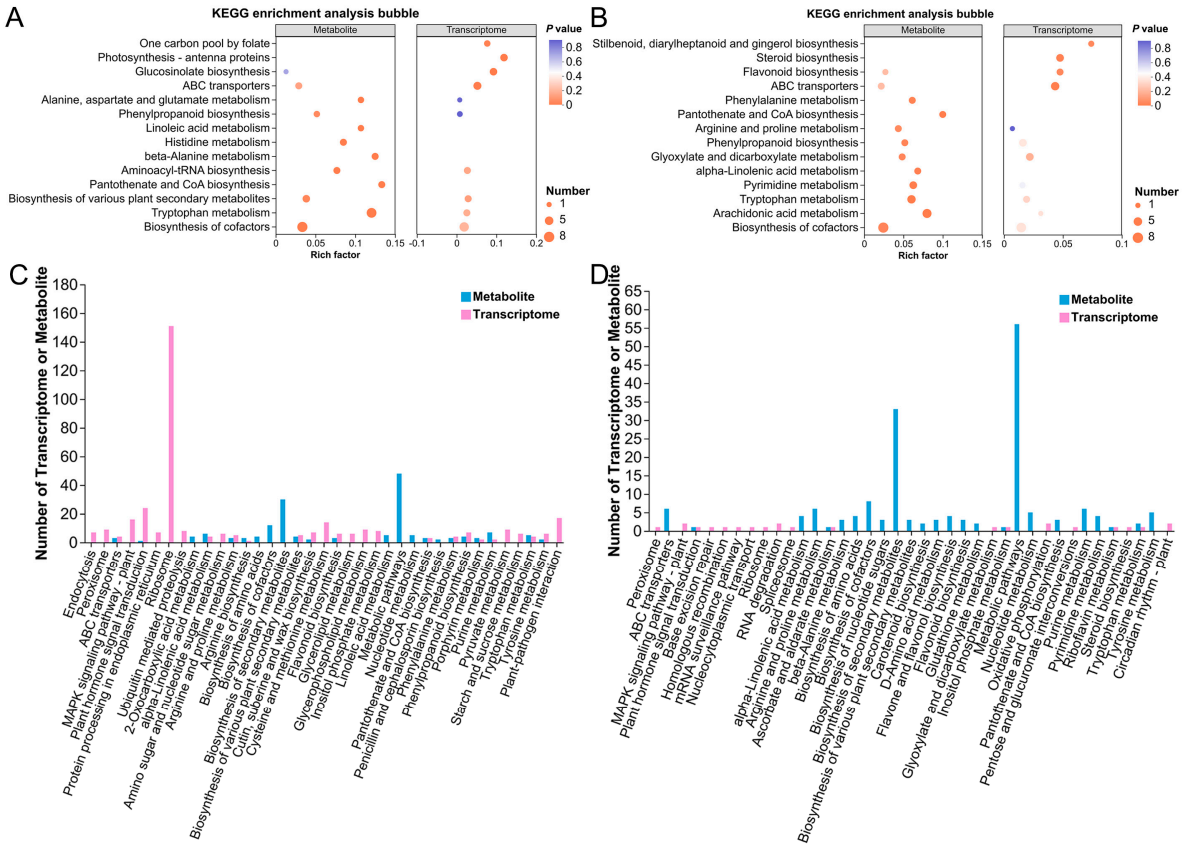


Figure 8. Metabolome and transcriptome analysis. (**A**) KEGG enrichment analysis bubble (CP628 vs. CP21). (**B**) KEGG enrichment analysis bubble (SD628 vs. SD21). The left panel shows the metabolome results, and the right panel displays the transcriptome results. Tertiary pathways with significant enrichment of genes and metabolites were screened by default, their union set was obtained, and the top 10 pathways were separately selected for plotting. (**C**) KEGG analysis of the metabolome and transcriptome in ZG-628. (**D**) KEGG analysis of the metabolome and transcriptome in ZG-21. The KEGG annotations of genes are displayed in pink, and the KEGG annotations of metabolites are displayed in blue.

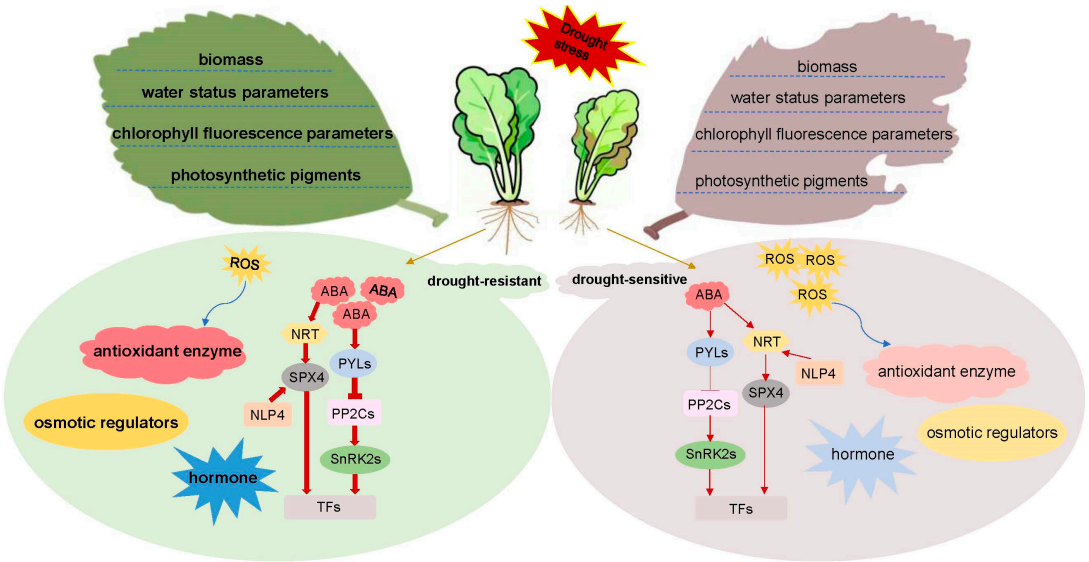


Figure 9. Response Mechanisms of Drought-Resistant and Susceptible Varieties under Drought Stress.

4. Discussion

As a globally important vegetable crop, cabbage is highly susceptible to drought stress, which limits its growth and yield [41]. Therefore, elucidating the physiological and molecular mechanisms underlying its drought tolerance is crucial for ensuring stable production and facilitating genetic improvement [48]. In this study, the drought-tolerant genotype 'ZG-628' and the drought-sensitive genotype 'ZG-21' were identified through systematic screening. By integrating physiological, transcriptomic, and metabolomic analyses, the study comprehensively revealed the potential regulatory network governing drought tolerance in cabbage, providing critical crucial insights for breeding drought-tolerant varieties and enhancing yield stability in arid regions [49].

Based on evaluations of drought resistance during the seed germination and seedling stages, 'ZG-628' and 'ZG-21' were selected from 29 cabbage materials. PEG-6000-simulated drought stress showed that the RGR and GDRI of 'ZG-628' were significantly higher than those of 'ZG-21' (Figure 1A,B), suggesting that drought-tolerant genotypes may initiate germination more rapidly, thereby establishing early growth advantages under water-limited conditions [50]. Growth indicators under well-watered conditions were also consistent with their drought tolerance (Figure 2A). Under drought stress, antioxidant enzyme activities (POD, SOD, and CAT) and osmoregulatory substance contents (such as proline and soluble sugars) were significantly higher in 'ZG-628' than in 'ZG-21', whereas MDA content was lower. These results indicate that 'ZG-628' enhances drought tolerance by synergistically improving ROS scavenging and osmoregulation, thereby mitigating membrane lipid peroxidation [51]. In addition, drought-tolerant genotypes often exhibit robust photosynthetic protection [52]. In this study, compared with 'ZG-21', 'ZG-628' alleviated damage to its photosynthetic apparatus under drought stress by maintaining higher chlorophyll content, photosystem II activity, and electron transport capacity. The significant differences in drought tolerance between these genotypes provide a solid foundation for further investigation into the molecular and physiological mechanisms of drought response in cabbage.

Transcriptome sequencing serves as a vital tool for systematically elucidating the molecular mechanisms underlying crop drought response and identifying key functional genes. The scale of the drought-responsive transcriptional reprogramming in 'ZG-628' was substantially greater than that in 'ZG-21' (with 1362 and 75 differentially expressed genes, respectively). Transcriptional reprogramming represents a core molecular mechanism for plant adaptation to drought, a process primarily orchestrated by the precise regulation of hormonal signaling pathways [53]. Within this framework, the expression of key components in the abscisic acid (ABA) signaling pathway underwent significant alterations: the expression of ABA receptor genes (e.g., PYL4, PYL6) was upregulated, while the expression of negative regulators such as type 2C protein phosphatases (PP2Cs) was likely suppressed, potentially leading to the activation of (SnRK2) and ultimately enhancing the expression of a suite of downstream stress-responsive genes [54]. Furthermore, the gene LOC106314351 (encoding an NRT1/PTR FAMILY 6.4-like protein) identified in this study may be involved in ABA hormonal regulation. This aligns with findings by Chu et al., which demonstrated that NRT1.1B can function as an ABA receptor and modulates ABA-mediated transcriptional responses through competitive binding with nitrate, enabling plants to integrate nutrient status and environmental signals [55]. These gene-level regulatory patterns correspond closely with the well-established role of the ABA signaling pathway in plant drought tolerance. In studies of other crop species [56,57], the PYL–SnRK2 signaling module has been confirmed to enhance drought resistance by improving stomatal regulation, facilitating the accumulation of osmotic solutes, and boosting oxidative stress tolerance. At the transcription factor level, the drought response in 'ZG-628'

was particularly pronounced. Multiple transcription factor genes from the WRKY and NAC families exhibited genotype-specific upregulation. These transcription factors act as key executors downstream of ABA signaling, playing a central role in regulating the expression of functional genes associated with antioxidant enzyme synthesis, osmotic adjustment, and water transport [58]. Their robust expression patterns are highly consistent with the physiological traits observed in 'ZG-628', namely its strong water retention capacity and minimal oxidative damage. Therefore, the drought tolerance of 'ZG-628' can be partly attributed to its enhanced ABA signal perception and transduction system, coupled with the precise regulation of the drought-responsive functional network by key downstream transcription factors [59].

Beyond transcriptional regulation, metabolic reprogramming also contributes significantly to drought tolerance in cabbage [60]. In particular, the specific accumulation of flavonoids constitutes a key component of the drought resilience in 'ZG-628'. Compared to the drought-sensitive 'ZG-21', 'ZG-628' exhibited a distinct accumulation of various flavonoids in leaves under stress, such as isorhamnetin-3-rutinoside-4′-rhamnoside, luteolin, and several quercetin derivatives. Concurrently, the "flavonoid and flavonol biosynthesis" pathway was specifically activated, as revealed by KEGG enrichment analysis. This metabolic signature strongly corresponded with the upregulation of key genes in this pathway from transcriptomic data, indicating that 'ZG-628' establishes a robust antioxidant defense through coordinated transcriptional and metabolic regulation [61]. This mechanism directly underpins its observed lower levels of oxidative damage (e.g., reduced MDA content) and better preservation of photosynthetic function (Figure 2). Therefore, the specific biosynthesis and accumulation of flavonoids in 'ZG-628' not only exemplifies the role of enhanced secondary metabolism in plant stress resistance [62] but also delineates a core metabolic route by which this genotype mitigates drought-induced oxidative stress and maintains cellular homeostasis. Notably, the metabolomic data further suggest crosstalk between different layers of the stress response. In 'ZG-628', not only was the level of the ABA hormone elevated, but certain ABA metabolic intermediates (e.g., dihydrophaseic acid, abscisic alcohol) also accumulated concomitantly [63]. At the same time, the flavonoid pathway was strongly induced. This implies that in 'ZG-628', enhanced ABA signaling, specifically activated secondary metabolism, and a reinforced antioxidant system may constitute a synergistic and interacting regulatory network, collectively consolidating its drought-tolerant phenotype.

Multi-omics joint analysis provides a powerful approach for unraveling the complex mechanisms of plant drought resistance, enabling the integration of physiological, transcriptional, and metabolic regulatory networks to comprehensively elucidate the molecular basis of genotypic variation [64]. In this study, integrated transcriptomic and metabolomic analyses revealed that the drought-tolerant genotype exhibited coordinated enrichment at both gene expression and metabolite accumulation levels in pathways such as plant hormone signal transduction, flavonoid biosynthesis, and cutin/suberin biosynthesis. For example, the upregulated expression of core components in the ABA signaling pathway (PYL-PP2C-SnRK2) and downstream transcription factors, including WRKY and NAC, corresponded closely with the significant accumulation of ABA in leaves and the specific increase in flavonoid metabolites. This concerted regulatory pattern between transcription and metabolism is consistent with previously reported multi-layered plant strategies for responding to drought stress. In species such as Medicago [65] and rice [66], the activation of the ABA signaling pathway is often accompanied by enhanced synthesis of secondary metabolites, collectively constituting forming an integrated plant defense network.

5. Conclusions

Through integrated physiological, transcriptomic, and metabolomic analyses, this study systematically revealed the differential response mechanisms of two cabbage genotypes under drought stress. Physiological characterization demonstrated that the drought-tolerant genotype 'ZG-628' maintained better water status, antioxidant activity, and photosynthetic performance, whereas the drought-sensitive genotype 'ZG-21' exhibited more severe water loss, oxidative damage, and photosynthetic decline. Integrated transcriptomic and metabolomic analyses further indicated that drought resistance relies on the effective activation of the ABA signaling pathway and the coordinated regulation of its downstream network. In 'ZG-628', ABA receptors (PYLs), protein kinases (SnRK2s), and transcription factors such as WRKY and NAC were strongly induced, orchestrating key stress-response pathways including osmotic regulation, ROS scavenging, and flavonoid biosynthesis. In contrast, 'ZG-21' showed weaker induction of ABA-related genes and limited accumulation of prCCotective metabolites. Overall, this study systematically elucidates the physiological and molecular basis of drought tolerance in cabbage, providing critical theoretical guidance for the targeted breeding of drought-resistant varieties.

Supplementary Materials: The following supporting information can be downloaded at: https://www.mdpi.com/article/10.3390/horticulturae12020239/s1, https://www.ncbi.nlm.nih.gov/bioproject/PRJNA1418934 (accessed on 5 February 2026). Figure S1: (A) PCA of transcriptional profiles among four treatment groups; (B–E) GO Enrichment Analysis of DEGs. Figure S2: KEGG Annotation Analysis of DEGs. Figure S3: (A) Correlation Analysis of DEGs and DAMs (CP628 vs. CP21); (B) Correlation Analysis of DEGs and DAMs (SD628 vs. SD21); (C) Venn diagram of co-annotated KEGG pathways that were significantly enriched in either the metabolome or transcriptome of ZG-628 and ZG-21. Table S1: Sequencing data statistics table. Table S2: Transcriptome Functional Annotation Statistics Table. Table S3: Differentially Expressed Genes (DEGs) Count Statistics Table. Table S4: Important drought-responsive metabolites identified by PLS-DA in ZG-628. Table S5: Important drought-responsive metabolites identified by PLS-DA in ZG-21.

Author Contributions: Conceptualization, funding acquisition, J.L.; validation, investigation, data curation, writing-original draft, H.W.; project administration, supervision, formal analysis, Y.G.; methodology, resources, Y.C. All authors have read and agreed to the published version of the manuscript.

Funding: This research was funded by the Research and Application Demonstration of Key Technology Integration for the Cool-Season Vegetable Industry in the Liupan Mountain Area (2021YFD1600302).

Data Availability Statement: Data are contained within the article or the Supplementary Materials. Further inquiries can be directed to the corresponding author.

Conflicts of Interest: The authors declare no conflicts of interest.

References

1. Sato, H.; Mizoi, J.; Shinozaki, K.; Yamaguchi-Shinozaki, K. Complex plant responses to drought and heat stress under climate change. *Plant J.* **2024**, *117*, 1873–1892. [CrossRef]
2. Vicente-Serrano, S.M.; Peña-Angulo, D.; Beguería, S.; Domínguez-Castro, F.; Tomás-Burguera, M.; Noguera, I.; Gimeno-Sotelo, L.; El Kenawy, A. Global drought trends and future projections. *Philos. T. R. Soc. A* **2022**, *380*, 20210285. [CrossRef]
3. Gebrechorkos, S.H.; Sheffield, J.; Vicente-Serrano, S.M.; Funk, C.; Miralles, D.G.; Peng, J.; Dyer, E.; Talib, J.; Beck, H.E.; Singer, M.B.; et al. Warming accelerates global drought severity. *Nature* **2025**, *642*, 628–635. [CrossRef] [PubMed]
4. Yang, Y.; Ma, X.; Yan, L.; Li, Y.; Wei, S.; Teng, Z.; Zhang, H.; Tang, W.; Peng, S.; Li, Y. Soil–root interface hydraulic conductance determines responses of photosynthesis to drought in rice and wheat. *Plant Physiol.* **2023**, *194*, 376–390. [CrossRef] [PubMed]
5. Chen, Q.; Cao, X.; Nie, X.; Li, Y.; Liang, T.; Ci, L. Alleviation role of functional carbon nanodots for tomato growth and soil environment under drought stress. *J. Hazard. Mater.* **2022**, *423*, 127260. [CrossRef] [PubMed]
6. Raza, A.; Mubarik, M.S.; Sharif, R.; Habib, M.; Jabeen, W.; Zhang, C.; Chen, H.; Chen, Z.; Siddique, K.H.M.; Zhuang, W.; et al. Developing drought-smart, ready-to-grow future crops. *Plant Genome* **2023**, *16*, e20279. [CrossRef]

7. Dzinyela, R.; Hwarari, D.; Opoku, K.N.; Yang, L.; Movahedi, A. Enhancing drought stress tolerance in horticultural plants through melatonin-mediated phytohormonal crosstalk. *Plant Cell Rep.* **2024**, *43*, 272. [CrossRef]
8. Abbas, K.; Li, J.; Gong, B.; Lu, Y.; Wu, X.; Lü, G.; Gao, H. Drought stress tolerance in vegetables: The functional role of structural features, key gene pathways, and exogenous hormones. *Int. J. Mol. Sci.* **2023**, *24*, 13876. [CrossRef]
9. Shawon, R.A.; Kang, B.S.; Lee, S.G.; Kim, S.K.; Ju Lee, H.; Katrich, E.; Gorinstein, S.; Ku, Y.G. Influence of drought stress on bioactive compounds, antioxidant enzymes and glucosinolate contents of Chinese cabbage (*Brassica rapa*). *Food Chem.* **2020**, *308*, 125657. [CrossRef]
10. Wang, X.; Zhao, W.; Wei, X.; Sun, Y.; Dong, S. Molecular mechanism of drought resistance in soybean roots revealed using physiological and multi-omics analyses. *Plant Physiol. Biochem.* **2024**, *208*, 108451. [CrossRef]
11. Ayyaz, A.; Fang, R.; Ma, J.; Hannan, F.; Huang, Q.; Athar, H.-R.; Sun, Y.; Javed, M.; Ali, S.; Zhou, W.; et al. Calcium nanoparticles (ca-nps) improve drought stress tolerance in brassica napus by modulating the Photosystem II, nutrient acquisition and antioxidant performance. *NanoImpact* **2022**, *28*, 100423. [CrossRef]
12. Liu, H.; Song, S.; Zhang, H.; Li, Y.; Niu, L.; Zhang, J.; Wang, W. Signaling Transduction of ABA, ROS, and Ca^{2+} in Plant Stomatal Closure in Response to Drought. *Int. J. Mol. Sci.* **2022**, *23*, 14824. [CrossRef]
13. Zhao, Y.; Wang, S.; Ma, X.; He, Y.; Zhou, J.; Jiao, S.; Xun, J.; Kong, X.; Wu, X.; Bai, X. GmANKTM21 positively regulates drought tolerance and enhanced stomatal response through the MAPK signaling pathway in soybean. *Int. J. Mol. Sci.* **2024**, *25*, 6972. [CrossRef]
14. Liu, J.; Shi, X.; Zhang, Z.; Cen, X.; Lin, L.; Wang, X.; Chen, Z.; Zhang, Y.; Zheng, X.; Wu, B.; et al. Deep neural network-mining of rice drought-responsive TF-TAG modules by a combinatorial analysis of ATAC-Seq and RNA-Seq. *Plant Cell Environ.* **2025**, *48*, 5217–5235. [CrossRef]
15. Yu, Y.; He, L.; Wu, Y. Wheat WRKY Transcription factor TaWRKY24 confers drought and salt tolerance in transgenic plants. *Plant Physiol. Biochem.* **2023**, *205*, 108137. [CrossRef]
16. Zhang, J.; Huang, D.; Zhao, X.; Zhang, M.; Wang, Q.; Hou, X.; Di, D.; Su, B.; Wang, S.; Sun, P. Drought-responsive WRKY transcription factor genes IgWRKY50 and IgWRKY32 from iris germanica enhance drought resistance in transgenic arabidopsis. *Front. Plant Sci.* **2022**, *13*, 983600. [CrossRef]
17. Debnath, S.; Kant, A.; Bhowmick, P.; Malakar, A.; Purkaystha, S.; Jena, B.K.; Mudgal, G.; Rahimi, M.; Helal, M.M.U.; Hasan, R.; et al. The enhanced affinity of WRKY reinforces drought tolerance in *Solanum Lycopersicum* L.: An innovative bioinformatics study. *Plants* **2023**, *12*, 762. [CrossRef]
18. Li, C.; Yan, C.; Sun, Q.; Wang, J.; Yuan, C.; Mou, Y.; Shan, S.; Zhao, X. The bHLH transcription factor AhbHLH112 improves the drought tolerance of peanut. *BMC Plant Biol.* **2021**, *21*, 540. [CrossRef]
19. Gu, X.; Gao, S.; Li, J.; Song, P.; Zhang, Q.; Guo, J.; Wang, X.; Han, X.; Wang, X.; Zhu, Y.; et al. The bHLH transcription factor regulated gene OsWIH2 is a positive regulator of drought tolerance in rice. *Plant Physiol. Biochem.* **2021**, *169*, 269–279. [CrossRef]
20. Liang, Y.; Ma, F.; Li, B.; Guo, C.; Hu, T.; Zhang, M.; Liang, Y.; Zhu, J.; Zhan, X. A bHLH Transcription factor, SlbHLH96, promotes drought tolerance in tomato. *Hortic. Res.* **2022**, *9*, uhac198. [CrossRef]
21. Yang, C.; Huang, Y.; Lv, P.; Antwi-Boasiako, A.; Begum, N.; Zhao, T.; Zhao, J. NAC Transcription factor GmNAC12 improved drought stress tolerance in soybean. *Int. J. Mol. Sci.* **2022**, *23*, 12029. [CrossRef]
22. Sun, S.; Li, X.; Nie, N.; Chen, Y.; Gao, S.; Zhang, H.; He, S.; Liu, Q.; Zhai, H. Sweet potato NAC transcription factor NAC43 negatively regulates plant growth by causing leaf curling and reducing photosynthetic efficiency. *Front. Plant Sci.* **2023**, *14*, 1095977. [CrossRef]
23. Zhang, F.; Wu, J.; Sade, N.; Wu, S.; Egbaria, A.; Fernie, A.R.; Yan, J.; Qin, F.; Chen, W.; Brotman, Y.; et al. Genomic basis underlying the metabolome-mediated drought adaptation of maize. *Genome Biol.* **2021**, *22*, 260. [CrossRef]
24. Yadav, A.K.; Carroll, A.J.; Estavillo, G.M.; Rebetzke, G.J.; Pogson, B.J. Wheat drought tolerance in the field is predicted by amino acid responses to glasshouse-imposed drought. *J. Exp. Bot.* **2019**, *70*, 4931–4948. [CrossRef]
25. Dwivedi, A.K.; Singh, V.; Anwar, K.; Pareek, A.; Jain, M. Integrated transcriptome, proteome and metabolome analyses revealed secondary metabolites and auxiliary carbohydrate metabolism augmenting drought tolerance in rice. *Plant Physiol. Biochem.* **2023**, *201*, 107849. [CrossRef]
26. Hu, H.; Fei, X.; He, B.; Luo, Y.; Qi, Y.; Wei, A. Integrated analysis of metabolome and transcriptome data for uncovering flavonoid components of zanthoxylum bungeanum maxim. Leaves Under Drought Stress. *Front. Nutr.* **2022**, *8*, 801244. [CrossRef]
27. Guo, X.; Lv, L.; Zhao, A.; Zhao, W.; Liu, Y.; Li, Z.; Li, H.; Chen, X. Integrated transcriptome and metabolome analysis revealed differential drought stress response mechanisms of wheat seedlings with varying drought tolerance. *BMC Plant Biol.* **2025**, *25*, 571. [CrossRef]
28. Xu, D.; Ni, Y.; Zhang, X.; Guo, Y. Multiomic analyses of two sorghum cultivars reveals the change of membrane lipids in their responses to water deficit. *Plant Physiol. Biochem.* **2022**, *176*, 44–56. [CrossRef]
29. Mukherjee, A.; Dwivedi, S.; Bhagavatula, L.; Datta, S. Integration of light and aba signaling pathways to combat drought stress in plants. *Plant Cell Rep.* **2023**, *42*, 829–841. [CrossRef]

30. Liu, R.; Liang, G.; Gong, J.; Wang, J.; Zhang, Y.; Hao, Z.; Li, G. a potential aba analog to increase drought tolerance in arabidopsis thaliana. *Int. J. Mol. Sci.* **2023**, *42*, 8783. [CrossRef]
31. Fidler, J.; Graska, J.; Gietler, M.; Nykiel, M.; Prabucka, B.; Rybarczyk-Płońska, A.; Muszyńska, E.; Morkunas, I.; Labudda, M. PYR/PYL/RCAR receptors play a vital role in the abscisic-acid-dependent responses of plants to external or internal stimuli. *Cells* **2022**, *11*, 1352. [CrossRef]
32. Soma, F.; Takahashi, F.; Kidokoro, S.; Kameoka, H.; Suzuki, T.; Uga, Y.; Shinozaki, K.; Yamaguchi-Shinozaki, K. Constitutively active B2 raf-like kinases are required for drought-responsive gene expression upstream of ABA-Activated SnRK2 kinases. *Proc. Natl. Acad. Sci. USA* **2023**, *120*, e2221863120. [CrossRef]
33. Brunetti, C.; Sebastiani, F.; Tattini, M. Review: ABA, flavonols, and the evolvability of land plants. *Plant Sci.* **2019**, *280*, 448–454. [CrossRef]
34. Hussain, Q.; Asim, M.; Zhang, R.; Khan, R.; Farooq, S.; Wu, J. Transcription factors interact with ABA through gene expression and signaling pathways to mitigate drought and salinity stress. *Biomolecules* **2021**, *11*, 1159. [CrossRef]
35. Wang, L.; Tian, T.; Liang, J.; Li, R.; Xin, X.; Qi, Y.; Zhou, Y.; Fan, Q.; Ning, G.; Becana, M.; et al. A transcription factor of the NAC family regulates nitrate-induced legume nodule senescence. *New Phytol.* **2023**, *238*, 2113–2129. [CrossRef]
36. Collin, A.; Daszkowska-Golec, A.; Szarejko, I. Updates on the role of ABSCISIC ACID INSENSITIVE 5 (ABI5) and ABSCISIC ACID-RESPONSIVE ELEMENT BINDING FACTORs (ABFs) in ABA signaling in different developmental stages in plants. *Cells* **2021**, *10*, 1996. [CrossRef]
37. Marusig, D.; Tombesi, S. Abscisic acid mediates drought and salt stress responses in vitis vinifera—A Review. *Int. J. Mol. Sci.* **2020**, *21*, 8648. [CrossRef]
38. Wang, P.; Cao, W.; Yang, L.; Zhang, Y.; Fang, Z.; Zhuang, M.; Lv, H.; Wang, Y.; Cheng, S.; Ji, J. Glucosinolate biosynthetic genes of cabbage: Genome-wide identification, evolution, and expression analysis. *Genes* **2023**, *14*, 476. [CrossRef]
39. Barber, A.; Müller, C. Drought and subsequent soil flooding affect the growth and metabolism of savoy cabbage. *Int. J. Mol. Sci.* **2021**, *22*, 13307. [CrossRef]
40. Zhang, W.; Wang, L.; Zhang, L.; Kong, X.; Zhang, J.; Wang, X.; Pei, Y.; Jin, Z. H2S-mediated balance regulation of stomatal and non-stomatal factors responding to drought stress in Chinese cabbage. *Hortic. Res.* **2023**, *10*, uhac284. [CrossRef]
41. Eom, S.; Baek, S.-A.; Kim, J.; Hyun, T. Transcriptome analysis in chinese cabbage (*Brassica rapa* ssp. *pekinensis*) provides the role of glucosinolate metabolism in response to drought stress. *Molecules* **2018**, *23*, 1186. [CrossRef]
42. Hasanuzzaman, M.; Nahar, K.; Anee, T.I.; Khan, M.I.; Fujita, M. Silicon-mediated regulation of antioxidant defense and glyoxalase systems confers drought stress tolerance in *Brassica napus* L. *S. Afr. J. Bot.* **2018**, *115*, 50–57.
43. Li, L.; Li, H.; Wu, L.; Qi, H. Sulfur dioxide improves drought tolerance through activating Ca^{2+} signaling pathways in wheat seedlings. *Ecotoxicology* **2022**, *31*, 852–859. [CrossRef]
44. Zhang, X.; Cheng, Z.; Yao, W.; Gao, Y.; Fan, G.; Guo, Q.; Zhou, B.; Jiang, T. Overexpression of PagERF072 from poplar improves salt tolerance. *Int. J. Mol. Sci.* **2022**, *23*, 10707. [CrossRef]
45. Jing, D.; Liu, F.; Li, S.; Dong, Y. Synergistic effects of SAP and PGPR on physiological characteristics of leaves and soil enzyme activities in the rhizosphere of poplar seedlings under drought stress. *Front. Plant Sci.* **2024**, *15*, 1485362. [CrossRef]
46. Mohagheghian, B.; Saeidi, G.; Arzani, A. Phenolic compounds, antioxidant enzymes, and oxidative stress in barley (*Hordeum Vulgare* L.) genotypes under field drought-stress conditions. *BMC Plant Biol.* **2025**, *25*, 709. [CrossRef]
47. Stefanov, M.; Rashkov, G.; Borisova, P.; Apostolova, E. Sensitivity of the photosynthetic apparatus in maize and sorghum under different drought levels. *Plants* **2023**, *12*, 1863. [CrossRef]
48. Wang, G.; Xu, X.; Gao, Z.; Liu, T.; Li, Y.; Hou, X. Genome-wide identification of LEA gene family and cold response mechanism of BcLEA4-7 and BcLEA4-18 in non-heading chinese cabbage [*Brassica campestris* (Syn. *Brassica rapa*) Ssp. *Chinensis*]. *Plant Sci.* **2022**, *321*, 111291. [CrossRef]
49. Lee, Y.R.; Ko, K.S.; Lee, H.E.; Lee, E.S.; Han, K.; Yoo, J.Y.; Vu, B.N.; Choi, H.N.; Lee, Y.N.; Hong, J.C.; et al. CRISPR/Cas9-mediated HY5 gene editing reduces growth inhibition in Chinese cabbage (*Brassica rapa*) under ER stress. *Int. J. Mol. Sci.* **2023**, *24*, 13105. [CrossRef]
50. Saadaoui, W.; Tarchoun, N.; Msetra, I.; Pavli, O.; Falleh, H.; Ayed, C.; Amami, R.; Ksouri, R.; Petropoulos, S.A. Effects of drought stress induced by d-mannitol on the germination and early seedling growth traits, physiological parameters and phytochemicals content of tunisian squash (*Cucurbita maxima* Duch.) landraces. *Front. Plant Sci.* **2023**, *14*, 1215394. [CrossRef]
51. Ren, K.; Tang, T.; Kong, W.; Su, Y.; Wang, Y.; Cheng, H.; Yang, Y.; Zhao, X. Response of watermelon to drought stress and its drought-resistance evaluation. *Plants* **2025**, *14*, 1289. [CrossRef]
52. Chegini, S.N.; Jafarinia, M.; Ghotbi-Ravandi, A.A. Unraveling the impacts of progressive drought stress on the photosynthetic lightreaction of tomato: Assessed by chlorophyll-a fluorescence and gene expression analysis. *Cell Mol. Biol.* **2024**, *70*, 176–184. [CrossRef]
53. Gupta, A.; Rico-Medina, A.; Caño-Delgado, A.I. The physiology of plant responses to drought. *Science* **2020**, *368*, 266–269. [CrossRef]

54. Nolan, T.M.; Vukašinović, N.; Liu, D.; Russinova, E.; Yin, Y. Brassinosteroids: Multidimensional regulators of plant growth, development, and stress responses. *Plant Cell* **2020**, *32*, 295–318. [CrossRef]
55. Hsu, P.; Dubeaux, G.; Takahashi, Y.; Schroeder, J.I. Signaling mechanisms in abscisic acid-mediated stomatal closure. *Plant J.* **2021**, *105*, 307–321. [CrossRef]
56. Wang, Z.; Li, Z.; Zhou, X.; Lu, M.; Ma, Y.; Zhang, M.; Liu, Y.; Gai, Z.; Yang, K.; Ren, M.; et al. Saline-alkaline stress alters the drought resistance of maize through the ABA-PYL-SnRK2s signaling axis. *Plant Physiol. Biochem.* **2025**, *229*, 110659. [CrossRef]
57. González-Guzmán, M.; Rodríguez, L.; Lorenzo-Orts, L.; Pons, C.; Sarrión-Perdigones, A.; Fernández, M.A.; Peirats-Llobet, M.; Forment, J.; Moreno-Alvero, M.; Cutler, S.R.; et al. Tomato PYR/PYL/RCAR abscisic acid receptors show high expression in root, differential sensitivity to the abscisic acid agonist quinabactin, and the capability to enhance plant drought resistance. *J. Exp. Bot.* **2014**, *65*, 4451–4464. [CrossRef]
58. Li, T.; Li, B.; Wang, Y.; Xu, J.; Li, W.; Chen, Z.; Mou, W.; Xue, D. WRKY transcription factors in rice: Key regulators orchestrating development and stress resilience. *Plant Cell Environ.* **2025**, *48*, 8388–8406. [CrossRef]
59. Arroyo-Álvarez, E.; Chan-León, A.; Girón-Ramírez, A.; Fuentes, G.; Estrella-Maldonado, H.; Santamaría, J.M. Genome-wide analysis of WRKY and NAC transcription factors in *Carica papaya* L. and their possible role in the loss of drought tolerance by recent cultivars through the domestication of their wild ancestors. *Plants* **2023**, *12*, 2775. [CrossRef]
60. Ma, X.; Wang, W.; Zhang, J.; Jiang, Z.; Xu, C.; Zhu, W.; Shi, B.; Yang, W.; Su, H.; Wang, X.; et al. NRT1.1B acts as an abscisic acid receptor in integrating compound environmental cues for plants. *Cell* **2025**, *188*, 5231–5248.e20. [CrossRef]
61. Rao, M.J.; Feng, B.; Ahmad, M.H.; Tahir Ul Qamar, M.; Aslam, M.Z.; Khalid, M.F.; Hussain, S.; Zhong, R.; Ali, Q.; Xu, Q.; et al. LC-MS/MS-based metabolomics approach identified novel antioxidant flavonoids associated with drought tolerance in citrus species. *Front. Plant Sci.* **2023**, *14*, 1150854. [CrossRef]
62. Cao, X.; Hu, Y.; Song, J.; Feng, H.; Wang, J.; Chen, L.; Wang, L.; Diao, X.; Wan, Y.; Liu, S.; et al. Transcriptome sequencing and metabolome analysis reveals the molecular mechanism of drought stress in millet. *Int. J. Mol. Sci.* **2022**, *23*, 10792. [CrossRef]
63. Li, Y.; Chen, Y.; Chen, J.; Shen, C. Flavonoid metabolites in tea plant (*Camellia sinensis*) stress response: Insights from bibliometric analysis. *Plant Physiol. Biochem.* **2023**, *202*, 107934. [CrossRef]
64. Chen, Y.; Wu, J.; Ma, C.; Zhang, D.; Zhou, D.; Zhang, J.; Yan, M. metabolome and transcriptome analyses reveal changes of rapeseed in response to ABA signal during early seedling development. *BMC Plant Biol.* **2024**, *24*, 245. [CrossRef]
65. Kim, T.J.; Hwang, Y.J.; Park, Y.J.; Lee, J.S.; Kim, J.K.; Lee, M.-H. Metabolomics Reveals Lysinibacillus capsici TT41-Induced Metabolic Shifts Enhancing Drought Stress Tolerance in Kimchi Cabbage (*Brassica rapa* L. subsp. *pekinensis*). *Metabolites* **2024**, *14*, 87. [CrossRef]
66. Han, C.; Chen, G.; Zheng, D.; Feng, N. Transcriptomic and metabolomic analyses reveal that ABA increases the salt tolerance of rice significantly correlated with jasmonic acid biosynthesis and flavonoid biosynthesis. *Sci. Rep.* **2023**, *13*, 20365. [CrossRef]

Disclaimer/Publisher's Note: The statements, opinions and data contained in all publications are solely those of the individual author(s) and contributor(s) and not of MDPI and/or the editor(s). MDPI and/or the editor(s) disclaim responsibility for any injury to people or property resulting from any ideas, methods, instructions or products referred to in the content.